

**INSTITUTO TECNOLÓGICO DE BUENOS AIRES – ITBA**

**ESCUELA DE POSTGRADO**

# **SURFACTANT AND POLYMER RETENTION IN CHEMICAL ENHANCED OIL RECOVERY PROCESSES**

**AUTOR: De la Cruz Vivanco, Carlos Alberto (Leg. N° 103432)**

**TUTOR ACADÉMICO: Voirin, Jean-Marie (IFP School)**

**TUTOR EN LA EMPRESA: Hernandez Morales, Clara (BASF Alemania)**

**TRABAJO FINAL PRESENTADO PARA LA OBTENCIÓN DEL TÍTULO DE**

**MASTER IN RESERVOIR GEOSCIENCE AND ENGINEERING (IFP SCHOOL)**

**ESPECIALISTA EN PRODUCCIÓN DE PETRÓLEO Y GAS (ITBA)**

**BUENOS AIRES**

**PRIMER CUATRIMESTRE, 2017**





# Surfactant and Polymer Retention in Chemical Enhanced Oil Recovery Processes

by

De la Cruz Vivanco, Carlos Alberto

Company supervisor: Hernandez Morales, Clara

Academic supervisor: Voirin, Jean-Marie

Internship

at

**BASF**

Ludwigshafen am Rhein, Germany

to achieve the degree of

**Master in Reservoir Geoscience and Engineering**

at

**IFP School - École Nationale Supérieure du Pétrole et des Moteurs**  
Rueil-Malmaison, France

2017



## ACKNOWLEDGEMENTS

I would like to express my deepest gratitude to BASF for allowing me to spend four wonderful months doing this internship in Germany. I must also thank IFP School (France) and ITBA (Argentina) for giving me the opportunity to participate in this double-degree program which has given me the chance to grow as a professional and as a person. This has been a truly life-changing experience.

I must thank SPE Argentina and SPE Patagonia for trusting me and providing an honor loan for partial financial support to study in Rueil Malmaison.

I want to especially thank my supervisor at BASF, Dr. Clara Hernandez, for her guidance, for sharing her knowledge, experience and time, and for making me feel at home in a new country. I would also like to thank my supervisor at IFP School, Prof. Jean-Marie Voirin, for supporting me since the very beginning with the internship plan.

I am also thankful to Dr. Michael Büschel, Dr. Kathrin Cohen and Russell Giesbrecht for trusting in me to do the internship at BASF. I must also thank Dr. Stefan Stein, Dr. Edward Bohres, Dr. Adrian Villanueva, Dr. Gabriela Alvarez Juergenson, and Dr. Jack Tinsley for providing ideas, support and advice for my work.

I must dedicate a separate paragraph to express my gratitude to the laboratory technicians at BASF. Special thanks to Paola Kusch who worked so hard to obtain the results presented herein. I must also thank Bettina Drescher, Peter Imfeld, Florian Seitz, Dieter Puttner, Kristin Weber, Timo Weber, Tamara Kuelzer, and Dominic Bechen for all their help and support.

I am also indebted to the wonderful friends and colleagues I met at IFP School and ITBA, who have made this whole experience so much more joyful and happy. Now they are all spread around the world but I will keep them in my heart and I hope I can ever meet them again.

Last but not least, a big 'thank you' goes to the people I love the most and who are always there to support me, my family.



## CONTENTS

Acknowledgements .....	<i>iii</i>
Contents .....	<i>v</i>
Figures .....	<i>vi</i>
Tables .....	<i>vii</i>
Nomenclature .....	<i>viii</i>
Summary .....	<i>xi</i>
Objectives .....	1
Introduction .....	3
Retention mechanisms .....	4
Determination of surfactant and polymer concentration .....	7
Determination of surfactant concentration .....	7
Method S1: High performance liquid chromatography .....	7
Method S2: Two-phase titration with visual endpoint detection.....	8
Method S3: Potentiometric two-phase titration.....	9
Method S4: Potentiometric single-phase titration .....	9
Method S5: Extractive spectrophotometric method using methylene blue for anionic surfactants .....	10
Method S6: Extractive spectrophotometric method using TBPE for nonionic surfactants ....	11
Method S7: Organic matter content determination.....	11
Method S8: Spectrophotometric determination by UV absorption.....	12
Determination of polymer concentration .....	13
Method P1: Rheological determination using an isotorque curve .....	13
Method P2: Improved starch-iodide method .....	14
Method P3: Flocculation test.....	15
Method P4: Colloid titration .....	16
Method P5: Improved bleach method .....	17
Method P6: Organic matter content determination.....	17
Simultaneous determination of surfactant and polymer concentration .....	17
Introduction .....	17
Materials .....	22
Methodology .....	23
Results .....	24
Conclusions .....	29
Determination of surfactant and polymer retention.....	31
Determination of surfactant and polymer adsorption in static conditions .....	31

Introduction .....	31
Materials .....	31
Methodology .....	31
Results .....	33
Conclusions .....	36
Determination of surfactant and polymer retention in dynamic conditions .....	37
Introduction .....	37
Materials .....	37
Methodology .....	38
Results .....	39
Conclusions .....	47
Conclusions.....	49
References.....	51

## FIGURES

Figure 1. EOR decision-making workflow [2].....	3
Figure 2. Schematic diagram of retention mechanisms in porous media (adapted from Sorbie [28]). .....	5
Figure 3. Chromatograph of a sample containing different surfactants [31]. Ordinate: ELSD response. Abscissa: elution time.....	8
Figure 4. Typical titration curve of potentiometric two-phase titration [14].....	9
Figure 5. Typical titration curve of potentiometric single-phase titration [7].....	10
Figure 6. Calibration curve for anionic surfactant dodecyl benzene sulfonate (AS) according to the extractive spectrophotometric method using methylene blue [18].....	11
Figure 7. TOC calibration curve for an amphoteric surfactant (betaine) [23].....	12
Figure 8. UV absorption calibration curve for alkylbenzene sulfonate [23].....	13
Figure 9. Isotorque calibration curve for HPAM [24].....	14
Figure 10. Calibration curve of HPAM for the improved starch-iodide method [29].....	15
Figure 11. Transmittance duration curve and curve parameters, including clarity shift inflection (CSI) [22].....	15
Figure 12. Calibration curves for the flocculation test [22].....	16
Figure 13. Reaction between positive and negative polyelectrolytes [33]. ....	16
Figure 14. Determination of surfactant and polymer by single-variable regression approach. ....	21
Figure 15. Determination of surfactant and polymer by 2-variable regression approach. ....	22
Figure 16. Surfactant A calibration curve obtained by single-variable linear regression. ....	25
Figure 17. Surfactant B calibration curve obtained by single-variable linear regression. ....	25
Figure 18. Polymer A calibration curves obtained by single-variable linear regression.....	25



Figure 19. Polymer B calibration curves obtained by single-variable linear regression.....	26
Figure 20. Simultaneous determination of Surfactant A and Polymer A.....	27
Figure 21. Simultaneous determination of Surfactant A and Polymer B.....	28
Figure 22. Simultaneous determination of Surfactant B and Polymer A.....	29
Figure 23. Static adsorption experiment.....	33
Figure 24. Surfactant A adsorption isotherm at 23°C.....	34
Figure 25. Adsorption isotherm and model for the adsorption of non-ionic surfactant, showing the orientation of surfactant molecules at the surface [21]. .....	35
Figure 26. Polymer A adsorption isotherm at 23°C.....	35
Figure 27. Surfactant A adsorption isotherm at 23°C, with and without polymer.....	36
Figure 28. Simultaneous adsorption of Surfactant A and Polymer A at 23°C.....	36
Figure 29. Sandpack equipment.....	39
Figure 30. Permeability determination by flowrate variation for Surfactant A sandpack.....	40
Figure 31. Permeability determination by flowrate variation for Polymer A sandpack.....	41
Figure 32. Normalized injected and produced concentrations of Surfactant A during dynamic retention experiment.....	41
Figure 33. Cumulative mass of injected and produced Surfactant A during dynamic retention experiment.....	42
Figure 34. Cumulative mass of Surfactant A that remained inside the system during dynamic retention experiment.....	43
Figure 35. Normalized injected and produced concentrations of Polymer A during dynamic retention experiment.....	44
Figure 36. Cumulative mass of injected and produced Polymer A during dynamic retention experiment.....	45
Figure 37. Cumulative mass of Polymer A that remained inside the system during dynamic retention experiment.....	46

## TABLES

Table 1. Chemical structure of most common monomers in EOR polymers.....	19
Table 2. Chemical structure of most common EOR surfactants.....	20
Table 3. Synthetic sea water (SSW) composition.....	23
Table 4. Surfactant standard solutions.....	23
Table 5. Polymer standard solutions.....	24
Table 6. Surfactant-polymer standard solutions.....	24
Table 7. Calibration curves obtained by single-variable linear regression.....	25
Table 8. Calibration curves obtained by 2-variable linear regression.....	26
Table 9. Simultaneous determination of Surfactant A and Polymer A.....	27
Table 10. Simultaneous determination of Surfactant A and Polymer B.....	28

Table 11. Simultaneous determination of Surfactant B and Polymer A.....	29
Table 12. Surfactant solutions for static adsorption test.....	32
Table 13. Polymer solutions for static adsorption test.....	32
Table 14. Surfactant-polymer solutions for static adsorption test.....	32
Table 15. Maximum adsorption values observed at 23°C.....	37
Table 16. Sandpack properties.....	40
Table 17. Dynamic retention of Surfactant A in sandpack at 23°C.....	44
Table 18. Dynamic retention of Polymer A in sandpack at 23°C.....	47

## NOMENCLATURE

$A$	sandpack cross section area
$a_i$	surfactant concentration coefficient in $i$ -th calibration curve
ASP	alkali-surfactant-polymer
$b_i$	polymer concentration coefficient in $i$ -th calibration curve
$C_0$	initial surfactant/polymer concentration
$C_e$	equilibrium surfactant/polymer concentration
CEOR	chemical enhanced oil recovery
$c_i$	intercept in $i$ -th calibration curve
COD	chemical oxygen demand
CSI	clarity shift inflection time
CTAB	cetyltrimethylammonium bromide
$D$	sandpack diameter
$\Delta P$	pressure drop in sandpack
ELSD	evaporative light scattering detector
EO	ethylene oxide
EOR	enhanced oil recovery
$g$	gravity acceleration constant
$\Gamma$	surfactant/polymer adsorption per unit mass of rock/sand
$\Gamma_p$	polymer adsorption/retention per unit mass of rock/sand
$\Gamma_s$	surfactant adsorption/retention per unit mass of rock/sand
HPAM	partially hydrolyzed polyacrylamide
HPLC	high-performance liquid chromatography

IC	inorganic carbon
IFT	interfacial tension
$k$	permeability
$L$	sandpack column height
MIBK	methyl isobutyl ketone
$m_l$	liquid mass in static adsorption bottle
$m_s$	sand mass in static adsorption bottle or sandpack
$\mu$	viscosity
$[P]$	polymer concentration
$[P]_0$	injected polymer concentration
PAM	polyacrylamide
$[[P]]_i$	cumulative mass of injected polymer
$[[P]]_p$	cumulative mass of produced polymer
$\phi$	porosity
$P_{\text{loss}}$	pressure losses
PV or $V_p$	sandpack pore volume
$q$	flowrate
$\rho$	fluid density
$[S]$	surfactant concentration
$[S]_0$	injected surfactant concentration
$[[S]]_i$	cumulative mass of injected surfactant
$[[S]]_p$	cumulative mass of produced surfactant
SI	international system of units
SP	surfactant-polymer
SSW	synthetic sea water
TBPE	tetrabromophenolphthalein ethyl ester
TBPE-K	tetrabromophenolphthalein ethyl ester potassium salt
TC	total carbon
TDS	total dissolved solids
TN	total nitrogen
TOC	total organic carbon
$TOC_p$	polymer TOC

$TOC_s$	surfactant TOC
UV	ultraviolet
$V$	volume
$V_b$	sandpack bulk volume
$V_d$	system dead volume
$V_p$ or PV	sandpack pore volume

## SUMMARY

Chemical Enhanced Oil Recovery by alkali, surfactant and/or polymer flooding could be a good option to produce remaining oil from brown fields. One parameter that affects performance and economics of a CEOR process is how much of the injected chemicals is adsorbed or retained by the porous medium. There may be significant interactions between transported molecules and the porous medium which cause the chemical to be retained and lead to the formation of a bank of injection fluid wholly or partially denuded of chemical. Clearly, this can lead to a reduction in the efficiency of the chemical flood. Therefore, the level of chemical retention can be considered as one of the key factors in determining the economic viability of a chemical flood. Thus, it is of great importance to establish the correct retention levels for a given proposed field chemical EOR process. The conditions under which such laboratory measurements should be made are extremely important so that relevant figures for retention are available for the simulation assessment of the chemical flood.

In order to obtain relevant data for surfactant and polymer retention, reliable analytical methods must be available to determine their concentration. This is necessary to calculate retention by material balance in laboratory experiments or in the field. In this work, a bibliographic search was done to find analytical methods for surfactant and polymer determination. Several methods were found with good potential. Careful analysis of each methodology, equipment availability at BASF and previous experience, led to the conclusion that determination by Total Organic Carbon (TOC) and Total Nitrogen (TN) content was the most convenient option. It has the advantage that one single piece of equipment can analyze both TOC and TN and an autosampler can be used for automatic measurement. This makes it very convenient for retention determination experiments and coreflood tests in which many samples need to be analyzed. Therefore, this method was successfully implemented for determination of two surfactants and two polymers and calibration curves were obtained in the range from 0 to 200 ppm. Two calculation approaches were proposed for concentration determination, based on single- and two-variable linear regression. It was found that error is approximately 50% lower by using two-variable regression.

Once a reliable analytical method was implemented, experiments were carried out to determine surfactant and polymer retention onto Bentheimer sand in static no-flow conditions and in dynamic conditions in a sandpack, at 23 °C. One sulfate surfactant and one HPAM polymer from BASF were studied in synthetic sea water brine, with 3.5% TDS.

Adsorption isotherms obtained in static conditions showed that the surfactant was adsorbed in two layers, with maximum adsorption of 760  $\mu\text{g/g}$ . For the polymer, a maximum adsorption of 426  $\mu\text{g/g}$  was observed and possibly a two-layer adsorption behavior but further experiments are needed to confirm this. When both chemicals were mixed, competitive adsorption occurred and adsorption values decreased. Moreover, polymer prevented the adsorption of the second surfactant layer, reducing its adsorption by 80%.

Dynamic retention experiments were carried out with a 0.2-mL/min flowrate. Maximum amounts of 206 and 132  $\mu\text{g/g}$  were retained at 1500 ppm. This is only approximately 30% of the amount adsorbed in static conditions.

After water flooding, only 16.4% of previously adsorbed surfactant was desorbed, reaching a residual retention of 172  $\mu\text{g/g}$ . Regarding polymer, 31.7% was desorbed by water flooding, with a residual retention of 90  $\mu\text{g/g}$ . It can be said that retention is largely irreversible.



## OBJECTIVES

- Development of a laboratory methodology to determine surfactant and polymer concentration in Enhanced Oil Recovery formulations prepared in brine with different kinds of surfactants and polymers.
- Determination of surfactant and polymer adsorption onto solid adsorbent in static no-flow conditions.
- Determination of surfactant and polymer retention in porous media in dynamic conditions by chemical flooding of a sandpack.





## INTRODUCTION

Today fossil fuels supply more than 85% of the world's energy [26]. With global energy demand and consumption forecast to grow rapidly during the next 20 years, a realistic solution to meet this need relies in sustaining production from existing fields for several reasons:

- The industry cannot guarantee new discoveries.
- New discoveries are most likely to lie in offshore, deep offshore, or difficult-to-produce areas.
- Producing unconventional resources could be more expensive than producing from existing brown fields by Enhanced Oil Recovery methods.

Therefore, chemical EOR by alkali, surfactant and/or polymer flooding could be a good option to produce remaining oil from brown fields. However, there are only a few groups in well-recognized universities and companies that continue to develop, evaluate and understand the key features of EOR technologies today [2]. Unfortunately, oil price volatility has negatively impacted financial investments in EOR operations, leading to delays and, probably, missed opportunities when it comes to increasing oil recovery. EOR initiatives are often delayed because of either perceived or real financial risk.

Alvarado and Manrique [2] proposed an EOR decision-making workflow (Figure 1) which combines screening methods with reservoir simulation to support reservoir development plans and identify EOR opportunities.

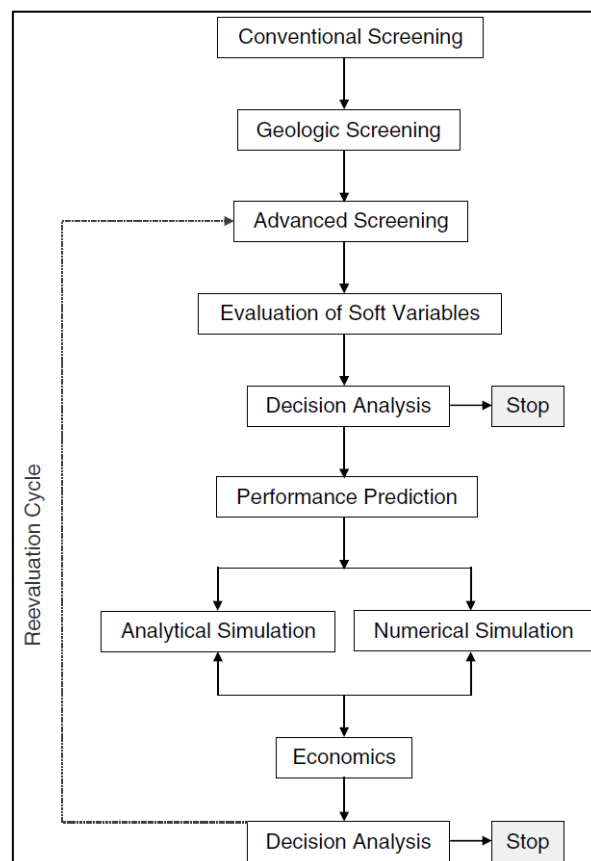


Figure 1. EOR decision-making workflow [2].

Based on the decision framework, predicting performance using analytical and/or numerical simulation is defined at early stages of the evaluation. Numerical simulation studies are costly and time consuming in addition to requiring highly trained professionals. In some cases, full numerical reservoir simulation studies are not justified because of the lack of available data and/or time constraints.

It is true that oil production forecasts obtained from analytical simulations tend to be overly optimistic, given their limitations. However, for fast screening purposes, analytical simulations provide key insights, sensible parameters, and a way to identify the uncertainties associated with different recovery processes. If projects do not offer economic merits using the optimistic production profiles in analytical simulations, most certainly the project economics will be less attractive when more detailed simulation studies are completed. In the case of numerical reservoir simulations, conceptual or sector models, instead of the full-field model, can be used to complete this step.

Economic model and calculations can be linked to simulations to help in decision analysis process.

One parameter that affects performance and economics of an EOR process is how much of the injected chemicals is adsorbed or retained by the porous medium. There may be significant interactions between transported molecules and the porous medium [28]. Such interactions will cause the chemical to be retained by the porous medium and will lead to the formation of a bank of injection fluid wholly or partially denuded of chemical. Clearly, this can lead to a reduction in the efficiency of the chemical flood. Therefore, the level of chemical retention can be considered as one of the key factors in determining the economic viability of a chemical flood. Thus, it is of great importance to establish the correct retention levels for a given proposed field chemical EOR process. The conditions under which such laboratory measurements should be made are extremely important so that relevant figures for retention are available for the simulation assessment of the chemical flood.

## Retention mechanisms

There are three retention mechanisms which are thought to act when surfactant/polymer solutions flow through porous media [28]. These are (Figure 2):

- Adsorption
- Mechanical entrapment
- Hydrodynamic retention

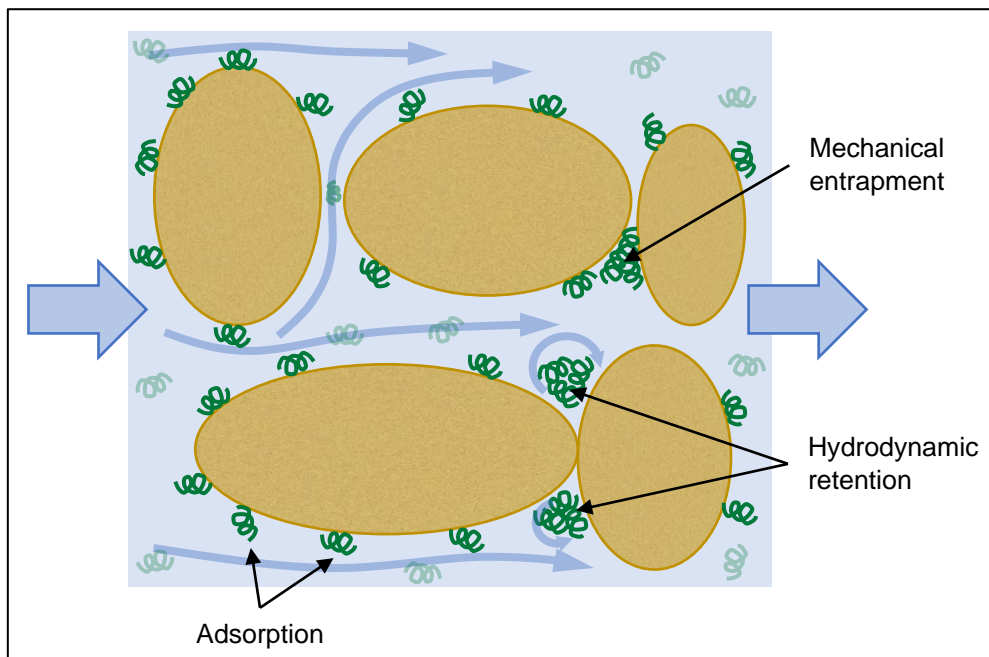


Figure 2. Schematic diagram of retention mechanisms in porous media (adapted from Sorbie [28]).

Adsorption is the main retention mechanism. It refers to the interaction between surfactant/polymer molecules and the solid surface, as mediated by the solvent. This interaction causes molecules to be bound to the surface of the solid mainly by physical adsorption (van der Waal's and hydrogen bonding). Essentially, surfactant/polymer occupies surface adsorption sites.

Mechanical entrapment is viewed as occurring when large molecules become lodged in narrow flow channels. When a solution is injected in a complex porous network, molecules take various routes and some can be trapped in the narrow pores. These block the flow and could probably cause further trapping of molecules. This retention mechanism is more likely to happen with large polymer molecules but not with surfactants.

In hydrodynamic retention, some of the molecules are temporarily trapped in stagnant flow regions by hydrodynamic drag forces. When the flow stops, these hydrodynamic forces disappear and molecules may diffuse out into the main flow channels.



## DETERMINATION OF SURFACTANT AND POLYMER CONCENTRATION

Several literature articles and standards were revised in order to find analytical methods which could be useful to determine surfactant and polymer concentration in effluents from laboratory coreflood tests and field EOR operations. These methods are necessary in order to determine how much of these chemicals is retained inside porous media.

### Determination of surfactant concentration

#### *Method S1: High performance liquid chromatography*

Surfactant concentration measurements can be done by High Performance Liquid Chromatography (HPLC). This technique can separate a mixture of compounds to identify and quantify the individual components in the mixture. A very small volume of the sample to be analyzed is injected into the stream of a mobile liquid phase. Then, the liquid flows through a porous column which contains a stationary solid phase. The chemical transport through the column depends on the physicochemical interactions of the surfactants in the sample with the stationary and mobile phases. Thus, depending on their chemical nature, some surfactants will have a higher tendency to be retained in the column than others, and individual components will elute at different times. By using an appropriate detector, the effluent can be analyzed and each surfactant in the sample can be identified and quantified.

For surfactant analysis, both ionic and nonionic, columns are available with special stationary phases that allow to separate individual components by using a mobile phase of organic solvent (usually acetonitrile) and water (with a pH buffer) with gradient elution technique.

For detection, UV absorbance detector can be used if the surfactants contain chromophore groups, e.g. benzene rings. However, this is not usually the case, thus the most widely used device for surfactants is Evaporative Light Scattering Detector (ELSD) [27]. The use of conductivity detector has also been reported [11].

Polymers used in EOR have been found to cause problems with the HPLC method because they can be retained in the chromatographic column, thus affecting its performance and shortening its lifetime. Therefore, sample pretreatment techniques have been developed to degrade the polymer before analysis, for example by use of sodium hypochlorite [27]. Also, the use of guard columns is recommended.

Figure 3 shows an example of a chromatograph obtained by HPLC [31]. It can be seen that it is possible to identify different surfactants in the sample and they can be quantified by measuring the areas under the peaks and using calibration curves of peak area vs surfactant concentration.

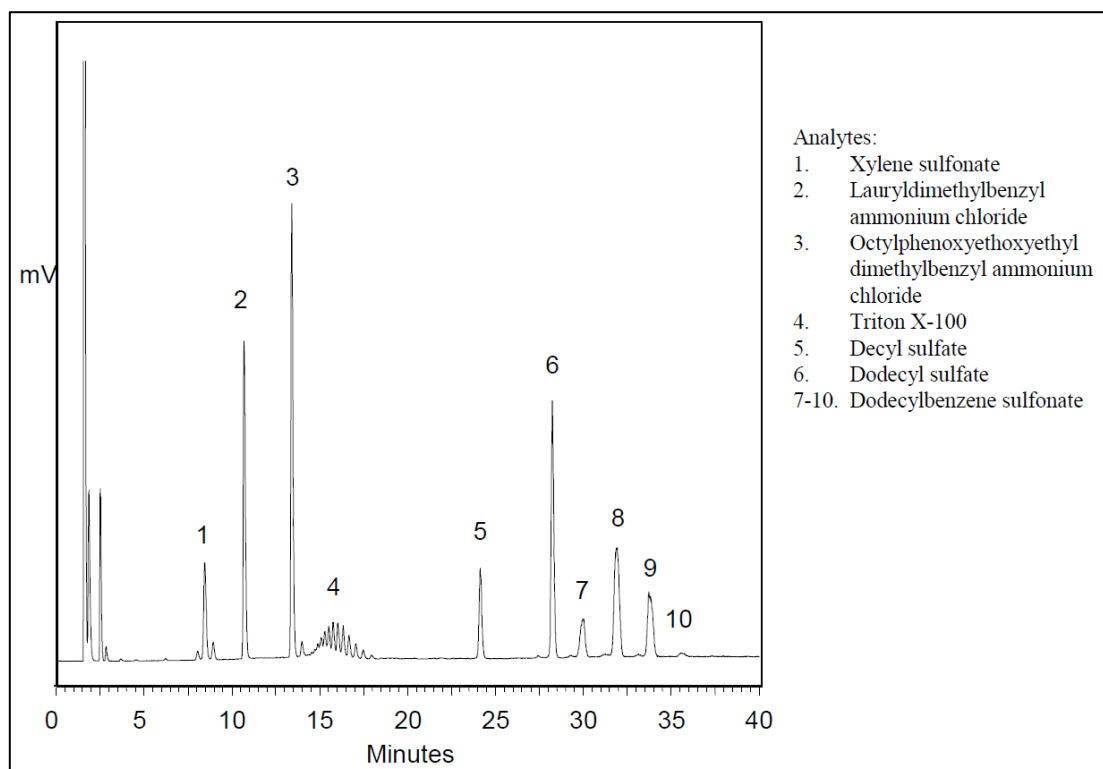


Figure 3. Chromatograph of a sample containing different surfactants [31]. Ordinate: ELSD response. Abscissa: elution time.

### Method S2: Two-phase titration with visual endpoint detection

This method allows to determine anionic surfactant concentration by titration with a cationic reagent which is usually Hyamine 1622, though other titrants have been used, such as cetyltrimethylammonium bromide (CTAB).

The titration occurs in a two-phase aqueous/organic-solvent system and the endpoint is detected visually by the use of specific color indicators. There are two possible approaches for visual endpoint detection:

1. Use of mixed indicator (dimidium bromide and disulphine blue) [6,15,17,35]. The anionic surfactant in the aqueous sample reacts with the cationic dye (dimidium bromide) to form a complex that is transferred to a chloroform phase, making this layer pink. As Hyamine is added as titrant, it reacts preferably with the anionic surfactant and the cationic dye is released back to the aqueous phase. After the equivalence point, an excess of Hyamine reacts with the anionic dye (disulphine blue) to form a chloroform-soluble blue complex. As a consequence, during the titration, the chloroform layer changes from pink, to gray, to blue. The gray color is taken as the endpoint.
2. Use of methylene blue [4]. The anionic surfactant in the aqueous sample reacts with the cationic indicator to form a complex which is transferred to a chloroform phase, making it blue. As CTAB is added as titrant (Hyamine 1622 may also be used), it reacts preferably with the anionic surfactant and the cationic dye is gradually released back to the aqueous layer. The endpoint is reached when the blue color has the same intensity in the two layers.

### **Method S3: Potentiometric two-phase titration**

Anionic surfactants are combined with cationic surfactants to form water-insoluble ion pairs, which are immediately extracted into a water immiscible organic solvent. This fundamental reaction is the basis for the titration of ionic surfactants with an oppositely charged surfactant standard solution. Thus anionic surfactants can be titrated with benzethonium chloride (Hyamine) [14] or cetylpyridinium chloride [34].

The titration process is supported by intensively stirring the two-phase mixture of aqueous solution and organic phase (methyl isobutyl ketone, MIBK) in order to maintain a stable emulsion. The potential which is formed in the emulsion during the titration, is recorded against the amount of titrant added with the help of a solvent-resistant surfactant-sensitive electrode in combination with a silver/silver-chloride reference electrode. The endpoint corresponds to the inflection point of the titration curve, as shown in Figure 4 [14].

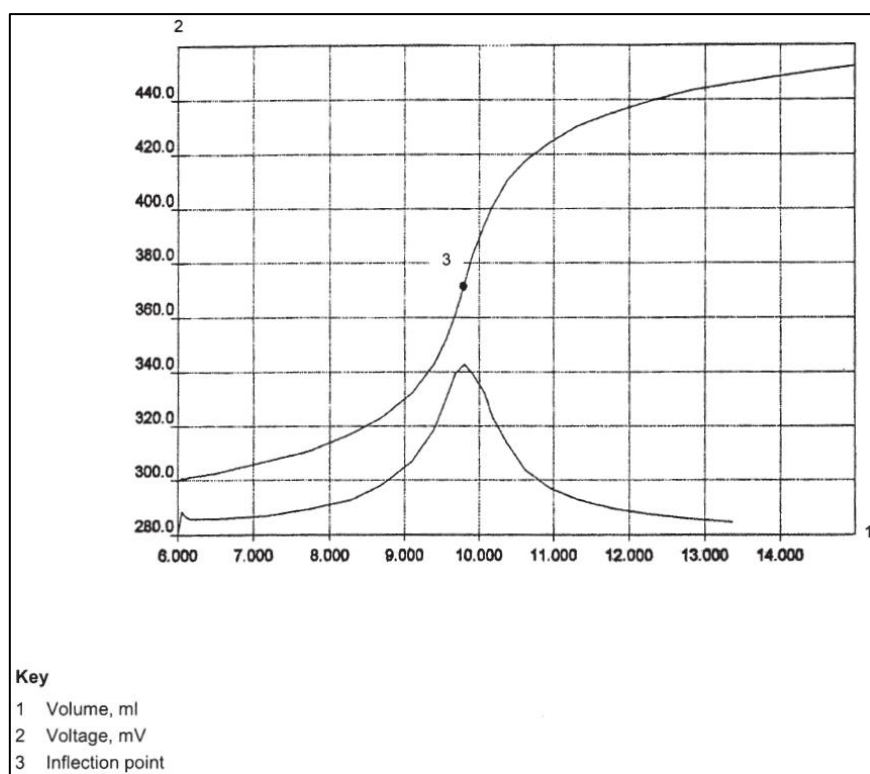


Figure 4. Typical titration curve of potentiometric two-phase titration [14].

In comparison to usual laboratory two-phase titration with visual endpoint determination, potentiometric titration offers the advantage of automation, operator-dependent differences in recognizing the equivalence point can be neglected, and a non-critical solvent replaces the toxicologically critical chloroform.

### **Method S4: Potentiometric single-phase titration**

Anionic surfactants can be determined by potentiometric titration with a cationic reagent, Hyamine 1622, in aqueous phase [7,8]. The titration reaction involves the formation of a complex between the cationic quaternary ammonium titrant and the anionic surfactant, which precipitates. A nitrate

ion-selective electrode and a Ag/AgCl reference electrode are used for measuring the potential of the aqueous solution. It is believed that the nitrate electrode responds to the concentration of unreacted anionic surfactant and that an excess of titrant generates a potential change large enough to give a well-defined inflection point in the titration curve at the endpoint (Figure 5).

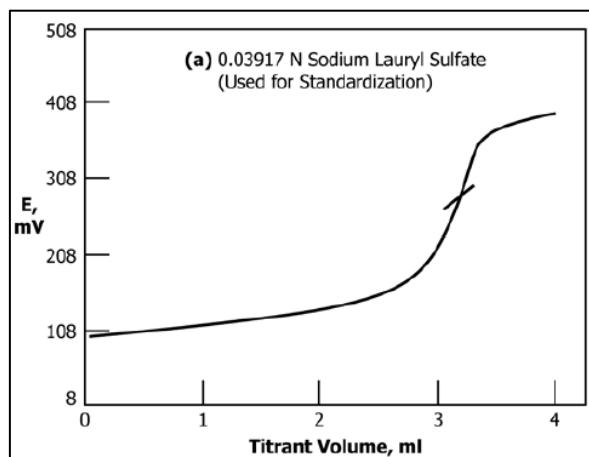


Figure 5. Typical titration curve of potentiometric single-phase titration [7].

Compared to Methods S2 and S3, this method has the advantage that it eliminates the use of an organic solvent, especially chloroform whose use is restricted for environmental and toxicological reasons.

#### **Method S5: Extractive spectrophotometric method using methylene blue for anionic surfactants**

The method is based on the formation of an ionic pair between the anionic surfactants in the sample and methylene blue, which is a cationic dye [18]. The ionic pair is insoluble in water and is extracted to a chloroform phase. The blue color intensity of the chloroform phase is related to the amount of anionic surfactant originally in the sample. Therefore, the anionic surfactant concentration can be determined by measuring absorbance at 650 nm and comparing with a calibration curve (Figure 6).

Since chloroform is denser than water, the analytical procedure can be conducted directly in a test tube suitable for spectrophotometric measurement. After the reaction and extraction occur with vigorous stirring, the system can be left at rest for 5 min to allow the chloroform phase to settle in the bottom. Afterwards, absorbance can be measured in the spectrophotometer without the need to remove the upper aqueous phase.



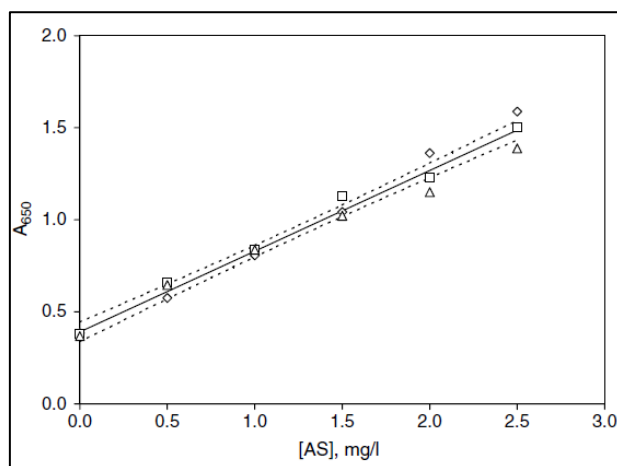


Figure 6. Calibration curve for anionic surfactant dodecyl benzene sulfonate (AS) according to the extractive spectrophotometric method using methylene blue [18].

### **Method S6: Extractive spectrophotometric method using TBPE for nonionic surfactants**

The polyoxyethylene chain in nonionic surfactants can trap potassium ions to form a complex cation [32]. This cation can react with an anionic dye, tetrabromophenolphthalein ethyl ester potassium salt (TBPE-K), to form an ionic pair which can be extracted into 1,2-dichloroethane or *o*-dichlorobenzene. TBPE provides a sensitive chromophore for subsequent spectrophotometric determination of the nonionic surfactant at a wavelength of 609 nm in the organic phase.

Since the organic phase is denser than water, the analytical procedure can be conducted directly in a test tube suitable for spectrophotometric measurement. After the reaction and extraction occur with vigorous stirring, the system can be left at rest for a few minutes to allow the organic phase to settle in the bottom. Afterwards, absorbance can be measured in the spectrophotometer without the need to remove the upper aqueous phase.

The biggest drawback of this method is that it is affected by high concentration of anionic surfactants.

### **Method S7: Organic matter content determination**

Surfactant concentration can be determined by measuring the amount of organic matter in the sample. In order to apply this methodology, surfactants must be the only organic species in the sample or the content of other organic species must be known in order to subtract them from the total organic content.

Two methodologies have been used by researchers to determine organic matter content in EOR fluid samples containing surfactants:

1. Total Organic Carbon (TOC) [1,23]. The concentration of surfactant is proportional to carbon content (Figure 7) thus TOC can be used to determine surfactant concentration. However, it is suggested to perform a background TOC measurement in order to subtract any additional organic matter that could be in the sample [23]. Moreover, a TOC baseline must be determined when organic additives are used [1].

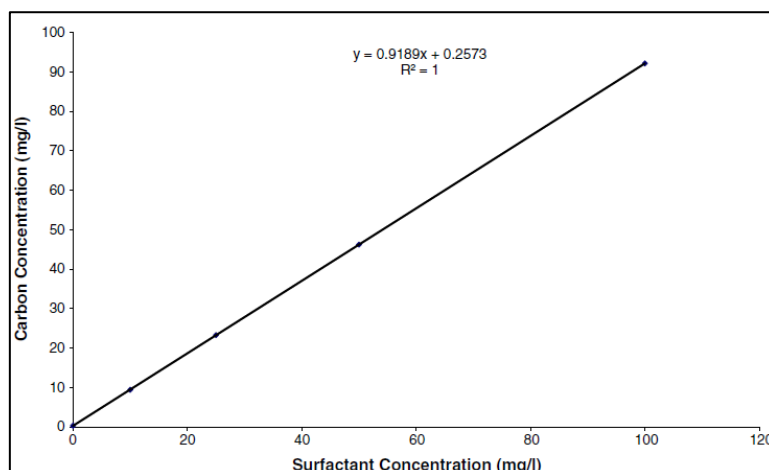


Figure 7. TOC calibration curve for an amphoteric surfactant (betaine) [23].

2. Chemical Oxygen Demand (COD) [10]. COD is an indirect way to measure the amount of organic compounds in an aqueous sample, thus it is proportional to surfactant content. The basis for the COD test is that nearly all organic compounds can be fully oxidized with a strong oxidizing agent (potassium dichromate) under acidic conditions. COD is the equivalent oxygen required to oxidize organic matter to carbon dioxide, ammonia and water. As it was suggested for TOC determination, a baseline COD should be determined in order to deduct other organic species that could be present in the sample. The most common interfering agent is chloride ion, which could be a problem in high salinity brines. This interference can be overcome largely, though not completely, by complexing with mercuric sulfate.

### **Method S8: Spectrophotometric determination by UV absorption**

Some surfactants contain chromophore groups in their chemical structures, such as benzene rings. In this case, surfactant concentration can be determined by measuring the ultraviolet absorbance of the sample at a wavelength of 224 nm and comparing with a calibration curve. Researchers have used this method to determine anionic surfactants [5,23] and nonionic surfactants [13,21].

Figure 8 shows an example of a calibration curve obtained for alkylbenzene sulfonate.

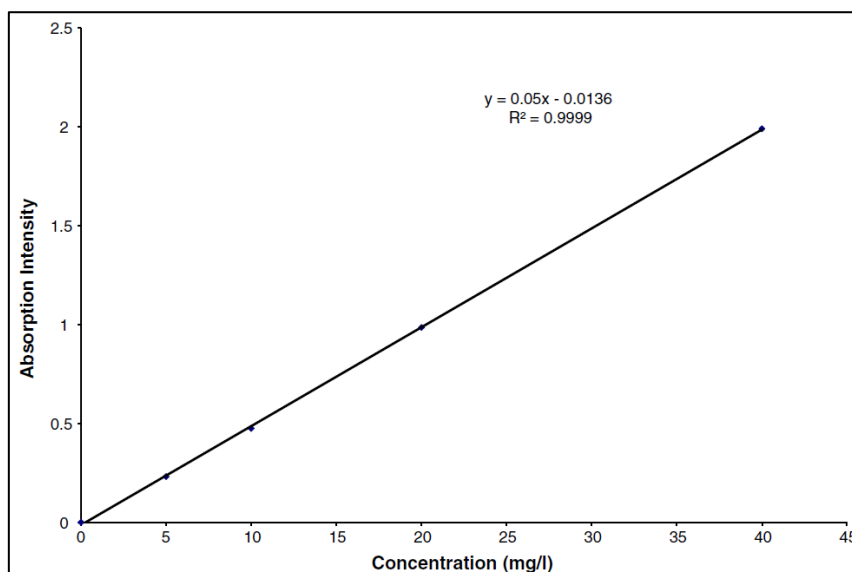


Figure 8. UV absorption calibration curve for alkylbenzene sulfonate [23].

This method is very convenient due to its simplicity but it is affected by the presence of amides, which also absorb in the UV range. Therefore, this method is not suitable for surfactant-polymer samples that contain polyacrylamides.

## Determination of polymer concentration

### **Method P1: Rheological determination using an isotorque curve**

Polymer concentration measurements can be done by rheological determination. However, there are usually two serious drawbacks:

1. Polymer degradation due to shear stress caused by flow through a porous medium can affect the results.
2. The precision of viscosity measurements is variable along the wide range of polymer concentrations that need to be determined and could be very low for samples with low concentration.

To solve the first drawback, Mezzomo et al [24] propose building a calibration curve with an effluent sample of known concentration, which has already undergone mechanical degradation in the porous medium. In the case of laboratory coreflood tests, this can be achieved by allowing the system to reach steady state, in which case the effluent concentration is the same as the injected concentration. In the case of field samples, another reliable polymer determination method can be used to determine the concentration in the effluent sample that will be used to build a calibration curve.

To solve the second drawback, the authors suggest not making the usual calibration curve of viscosity vs polymer concentration, but building a calibration curve of shear stress necessary to achieve a constant torque vs polymer concentration. This procedure ensures a constant precision for the entire range of concentration measurements. Figure 9 shows an example of the calibration curves found by the authors.

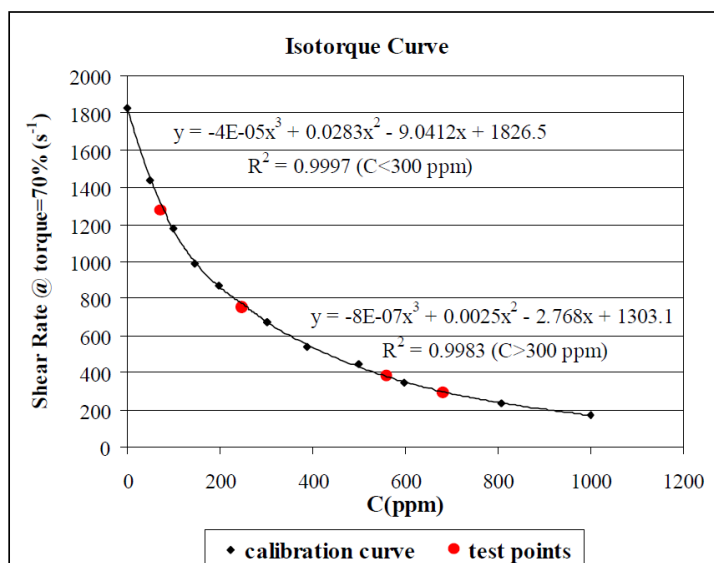


Figure 9. Isotorque calibration curve for HPAM [24].

The authors tested the method for HPAM in a concentration range of 0-1000 ppm and found a maximum error of 8%. In comparison with the bleach spectrophotometric method [3] they found the calibration curves of the isotorque method have better correlation coefficients and the results show higher precision.

### **Method P2: Improved starch-iodide method**

This method, published by Taylor [29], is an improvement to the starch-iodide method presented in API RP 63 standard [3], which allows the measurement of HPAM concentration in samples that contain surfactants. Also, the author explains a way to do an automated determination by flow injection analysis which allows to analyze 90 samples/hour.

The method is based on the formation of an N-bromo amide by reaction of the amide group of polyacrylamide with bromine. Excess bromine is removed by reaction with sodium formate. The N-bromo amide then converts iodide to iodine which is measured spectrophotometrically as the starch-triiodide complex.

The author applied a modification to the starch-cadmium iodide reagent by adding a surfactant. Triton X-100 (non-ionic surfactant), sodium dodecyl sulfate and Neodol 25-3S (sodium dodecylpoly(oxyethylene)-ether sulfate) were evaluated. A shift in the wavelength corresponding to maximum absorbance was observed in the three cases and intensity was also affected. At surfactant concentrations above 0.5 g/L, these parameters stabilized. Consequently, a concentration of 1 g/L surfactant was used in the reagent, and measurements were made at an adequate wavelength. This modification had the result of greatly reducing surfactant interference in the method.

Figure 10 shows a calibration curve found by the author. It was found that HPAM can be determined in the range of 0.5-75 mg/L, with good reproducibility (relative standard deviation less than 1.5%).

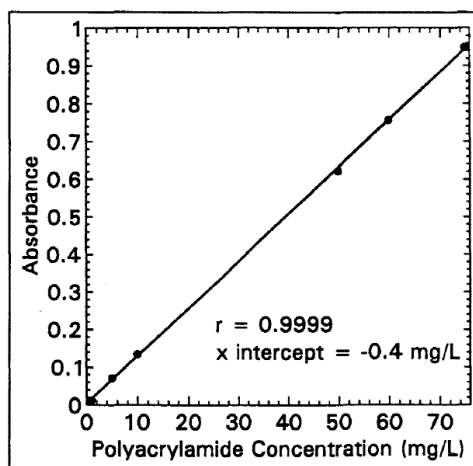


Figure 10. Calibration curve of HPAM for the improved starch-iodide method [29].

### Method P3: Flocculation test

Lentz et al [22] developed a method to measure PAM concentration in irrigation water. A kaolinite mineral standard is mixed with the sample containing polymer. As a result, flocculation occurs, which makes the sample turbid. Immediately after agitating, the sample transmittance is recorded as a function of time, Figure 11. Sample transmittance remains very low during Phase I. Once the floccules start to settle, the suspension begins to clear and sample transmittance increases abruptly. This time, which marks the beginning of Phase II, was called the clarity shift inflection (CSI) and the authors found that it is highly correlated to PAM concentration.

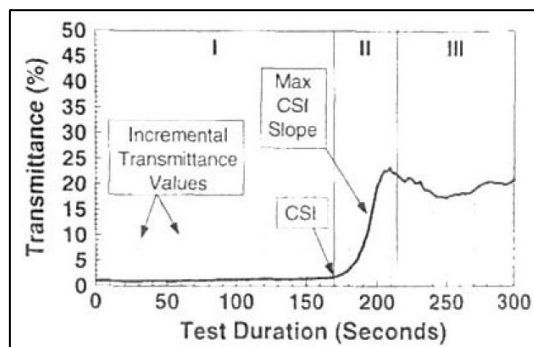


Figure 11. Transmittance duration curve and curve parameters, including clarity shift inflection (CSI) [22].

Figure 12 shows calibration curves of CSI vs polymer concentration, obtained by the authors for the ranges of 0-2.5 mg/L and 2.5-10 mg/L PAM. They found an average error of 10% for the high concentration range determination.

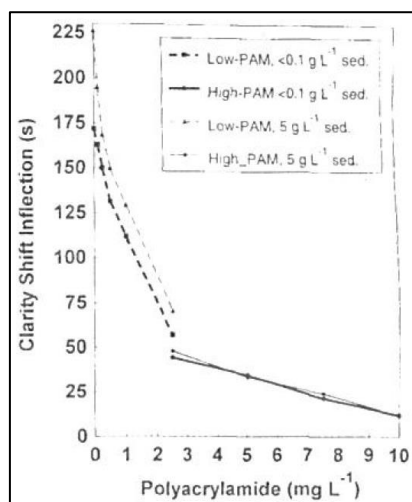


Figure 12. Calibration curves for the flocculation test [22].

#### Method P4: Colloid titration

This is a volumetric method for the determination of charged polyelectrolytes, like anionic polymers used in EOR. It is based on the reaction of positively charged polyelectrolytes and the negatively charged ones. When an aqueous solution containing a positive polyelectrolyte is added to an aqueous solution containing a negatively charged one, a neutralization reaction occurs stoichiometrically and a precipitate is formed (Figure 13). Therefore, if the positive polyelectrolytes whose chemical structures, molecular weight or equivalent weight are known are selected as a titrant, the negative polyelectrolytes in the sample solution can be determined volumetrically as long as a method for detecting the equivalence point is available [33].

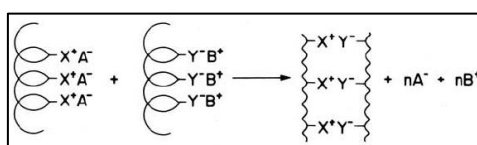


Figure 13. Reaction between positive and negative polyelectrolytes [33].

Ueno and Kina [33] propose several methods for endpoint determination:

- Use of visual indicators
- Electrochemical endpoint detection
  - Conductometric method, based on the change of conductivity of the solution during titration.
  - Use of ion-selective electrodes. In the titration of negative polyelectrolytes with positive polyelectrolyte, a trace amount of iodide ion can be added as an indicator ion, whose activity can be followed by the use of an iodide electrode. Iodide activity decreases suddenly after the equivalence point.
- Turbidimetric method. During the course of colloid titration, the solution becomes turbid, resulting in the sudden decrease of light transmittance at the endpoint.

As the colloid titration is based on the charge neutralization of polyelectrolytes, the presence of other electrolytes in the titration solution may interfere seriously. This interference could be caused, for example by high saline content and ionic surfactants.

### ***Method P5: Improved bleach method***

Kuehne and Shaw [20] developed an analytical method for measuring polyacrylamide concentration in the presence of sulfonate surfactants, which is based on the bleach method presented in API RP 63 standard [3]. Petroleum sulfonates cause interference with the original method. This interference was eliminated by the addition of an extraction step to remove sulfonates.

This is a turbidimetric method in which polyacrylamide polymer reacts with sodium hypochlorite in acetic acid to form an insoluble chloroamide. The resulting turbidity is proportional to polymer concentration and can be measured with a spectrophotometer or turbidimeter. If petroleum sulfonates are present in the samples, they are previously extracted with 1-butanol that is acidified with HCl. The HCl is necessary to change the sulfonates into sulfonic acids, so that they can be extracted easily. To prevent excess HCl from interfering with the polyacrylamide reaction, buffered acetic acid is used before reaction with sodium hypochlorite.

The authors were able to automate the method, with a throughput of 20-30 samples per hour. They achieved an accuracy of 5% in the polymer concentration range from 10 to 1200 ppm.

### ***Method P6: Organic matter content determination***

As well as surfactants, polymers can also be determined by measuring the amount of organic matter in the sample. In order to apply this methodology, polymer must be the only organic species in the sample or the content of other organic species must be known in order to subtract them from the total organic content.

Many authors have been able to determine polymer concentration through organic matter content determination by TOC [16,25,37] or COD [19]. These two methodologies were explained in Method S7 (page 11) for surfactants; the same principle applies to polymers. In addition, polymers can be determined by total nitrogen content analysis (TN) if they contain nitrogen atoms in their structure, like polyacrylamides.

## **Simultaneous determination of surfactant and polymer concentration**

### ***Introduction***

Total Organic Carbon (TOC) and Total Nitrogen (TN) measurements have been used by several researchers to determine the concentration of EOR polymers and surfactants in samples coming from coreflood tests [1,16,23,25,36,37].

In this method, the liquid sample enters a combustion furnace where all carbon-containing components are oxidized by oxygen (purified air) in presence of a catalyst, thus generating carbon dioxide. Then, the combustion gas is analyzed with a suitable CO<sub>2</sub>-detector to determine Total Carbon (TC) in the sample. On the other hand, an acidified sample is sparged with purified air to convert carbonate and bicarbonate into CO<sub>2</sub>, which is analyzed to determine Inorganic Carbon (IC) in the sample. Subtracting the IC concentration from the TC concentration determines the TOC content.

Using the same principle, the sample is oxidized in a combustion furnace with a catalyst to convert all nitrogen into nitrogen monoxide, which can be detected to determine TN in the sample.

By connecting carbon-dioxide and nitrogen-monoxide detectors in series, TOC and TN can be determined simultaneously from a single sample injection into the analyzer.

The main advantage of this method is its simplicity. However, any organic compound in the sample will be measured by TOC and many components could also be measured by TN, making it necessary to find a way to differentiate TOC and TN coming from different components in the sample. An effluent sample from a coreflood test or from an EOR field application could contain the following compounds that add up to TOC and/or TN:

- Surfactant
- Polymer
- Oil
- Additives

If a good oil/water phase separation is achieved, the effect of oil can be neglected. The effect of additives can be deducted by doing a TOC/TN baseline measurement, as suggested in literature [1,23]. This consists in analyzing a base sample with additives but without the chemicals to be determined (polymer, surfactants). The TOC/TN value of the base sample can be subtracted from the total TOC/TN of the bulk sample in order to obtain the TOC/TN concentration that strictly corresponds to the chemicals that are to be determined.

Once the TOC corresponding to the mixture of polymer and surfactant to be determined is known, it is necessary to determine one of these components by another method in order to calculate the other component by material balance. For example, some researchers have used the two-phase titration method to determine surfactant concentration [16,36] and then calculate polymer concentration by subtracting the surfactant from the TOC value of the sample.

In this work, it is proposed to use TN value to determine polymer concentration and then calculate surfactant concentration by material balance, using the TOC value. This is based on the fact that, for the most common chemicals used in EOR, nitrogen is only present in polymer but not in surfactants (Table 1 and Table 2). Therefore, TN value will be representative of polymer content, while TOC will be representative of both polymer and surfactant, since both compounds contain carbon.



Table 1. Chemical structure of most common monomers in EOR polymers.

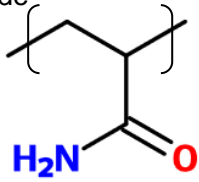
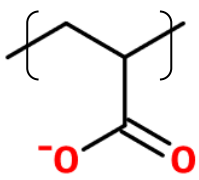
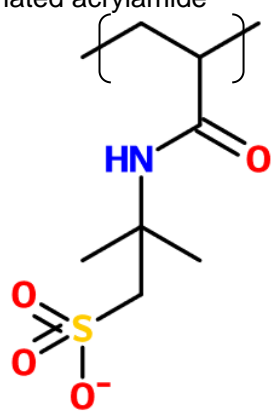
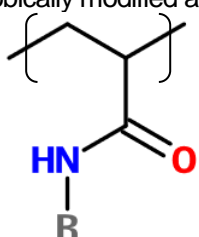
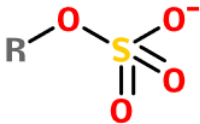
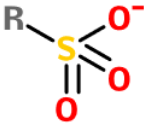
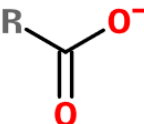
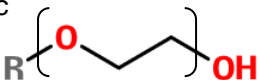
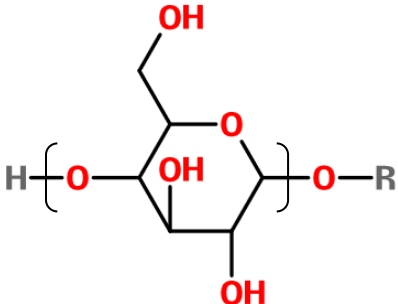
Monomer	Number of carbon and nitrogen atoms per monomer unit	Mass content of carbon and nitrogen
Acrylamide 	C: 3 N: 1	C: 50.7% N: 19.7%
Acrylate 	C: 3 N: 0	C: 38.3% N: 0.0%
Sulfonated acrylamide 	C: 7 N: 1	C: 36.7% N: 6.1%
Hydrophobically modified acrylamide 	C: depends on R chain N: 1	Depends on R chain

Table 2. Chemical structure of most common EOR surfactants.

Surfactant	Number of carbon and nitrogen atoms per molecule
Sulfate 	C: depends on R chain N: 0
Sulfonate 	C: depends on R chain N: 0
Carboxylate 	C: depends on R chain N: 0
Nonionic 	C: depends on R chain and number of EO groups N: 0
Alkylpolyglucoside 	C: depends on R chain and number of glucoside groups N: 0

Considering the chemical structures presented in Table 1, a standard polyacrylamide with 30% anionicity (70 mol% acrylamide, 30 mol% sodium acrylate) will have carbon and nitrogen mass fractions of 46.2% and 12.6%, respectively. Thus, a 100-ppm polymer solution will contain 46.2 ppm TOC and 12.6 ppm TN. Since nitrogen content is much lower than carbon content, it could be difficult to achieve accurate polymer concentration determinations from TN measurements in the lower range. For this reason, a TN vs polymer concentration calibration curve should be obtained in the laboratory in order to find the detection limit.

If polymer determination by TN is feasible for the desired concentration range, surfactant and polymer can be determined in an aqueous sample by simultaneous TOC and TN measurements. There are two possible approaches for concentration calculation which require different sets of standard solutions to obtain calibration curves:

- Single-variable regression. Standard solutions of surfactant alone and polymer alone are used to obtain calibration curves. In this work, 14 standard samples were used for each surfactant-polymer pair.
- 2-variable regression. Standard solutions of mixtures of surfactant and polymer are used to obtain calibration curves. In this work, 22 standard samples were used for each surfactant-polymer pair.

### Single-variable regression approach

This approach uses three calibration curves obtained by single-variable linear least-squares regression:

$$TN = b_1 [P] + c_1 \quad (1)$$

$$TOC_P = b_2 [P] + c_2 \quad (2)$$

$$TOC_S = a_3 [S] + c_3 \quad (3)$$

Once a sample is analyzed, and TOC and TN are known, Equation 1 can be used to calculate polymer concentration directly from TN value. Then,  $TOC_P$  can be obtained by using Equation 2 and  $TOC_S$  can be determined by material balance (Equation 4). Finally, surfactant concentration can be calculated from Equation 3. The calculation procedure is illustrated in Figure 14.

$$TOC_S = TOC - TOC_P \quad (4)$$

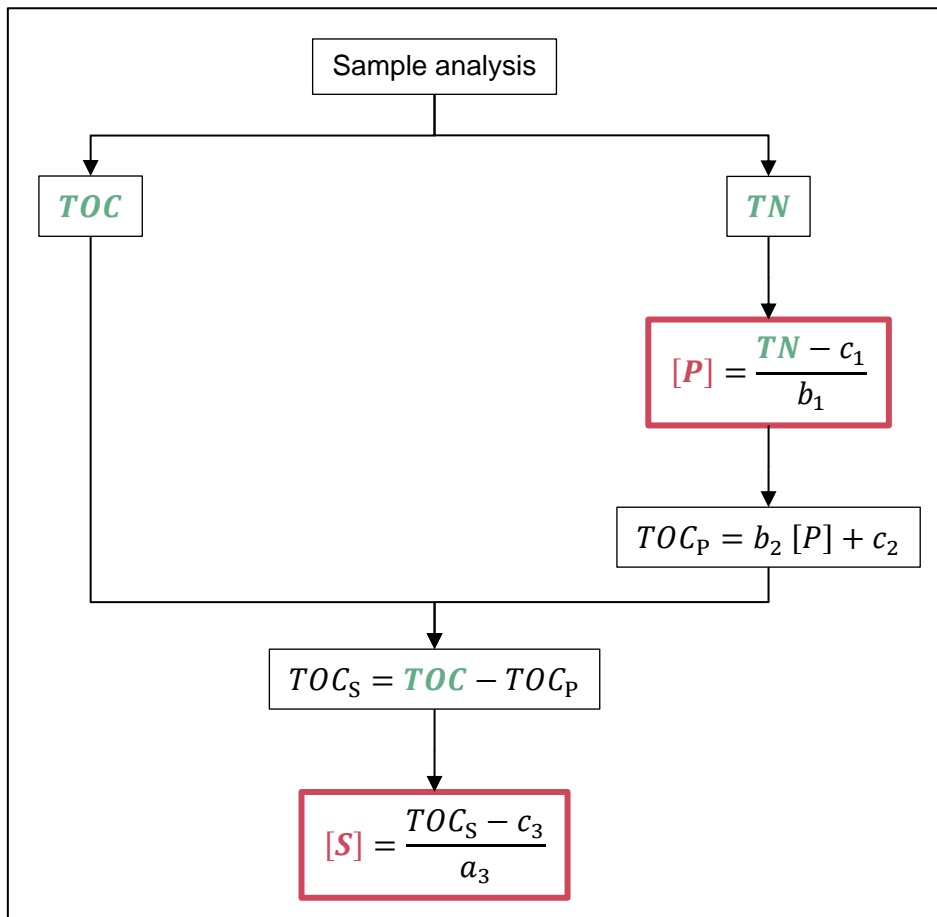


Figure 14. Determination of surfactant and polymer by single-variable regression approach.

### 2-variable regression approach

This approach uses two calibration curves obtained by 2-variable linear least-squares regression:

$$TN = b_4 [P] + c_4 \quad (5)$$

$$TOC = a_5 [S] + b_5 [P] + c_5 \quad (6)$$

Note that, even though a 2-variable approach is being considered, TN is only a function of polymer concentration (Equation 5) because it is the only component that contains nitrogen.

Once a sample is analyzed and TOC and TN are known, Equation 5 can be used to calculate polymer concentration directly from TN value. Then, surfactant concentration can be determined from Equation 6. The calculation procedure is illustrated in Figure 15.

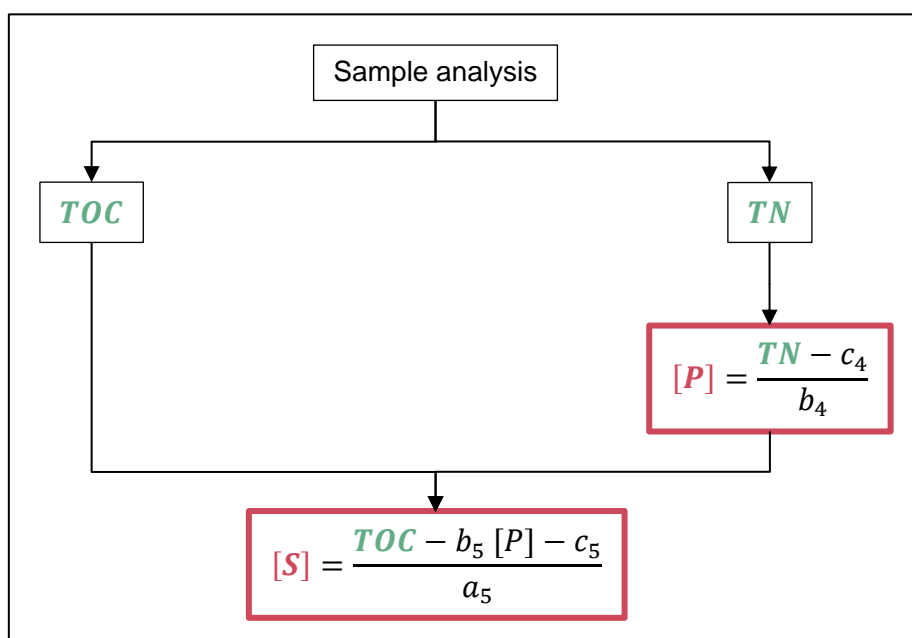


Figure 15. Determination of surfactant and polymer by 2-variable regression approach.

### Materials

Surfactants:

- Surfactant A (sulfate)
- Surfactant B (carboxylate)

Polymers:

- Polymer A (HPAM)
- Polymer B (thermally-stabilized HPAM)

Brine:

- Synthetic sea water (SSW), with composition detailed in Table 3.

Table 3. Synthetic sea water (SSW) composition.

Salt	Concentration (g/L)
Na <sub>2</sub> SO <sub>4</sub>	3.408
NaHCO <sub>3</sub>	0.168
KCl	0.746
MgCl <sub>2</sub> ·6H <sub>2</sub> O	9.149
CaCl <sub>2</sub> ·2H <sub>2</sub> O	1.911
NaCl	23.500

### Methodology

Standard solutions of surfactant and/or polymer were prepared in SSW brine to obtain calibration curves for both calculation approaches, single- and 2-variable regression. The concentration range was chosen from 0 to 200 ppm. This ensured that the samples were not too viscous for the TOC/TN analyzer auto-sampler. If higher concentrations were to be measured in the future, dilution would be necessary.

Surfactant-alone and polymer-alone standards were prepared with the compositions shown in Table 4 and Table 5. These were used for the single- and the 2-variable approach.

Standard solutions with mixtures of surfactant and polymer were prepared with the compositions shown in Table 6 for the pairs 'Surfactant A + Polymer A,' 'Surfactant A + Polymer B,' and 'Surfactant B + Polymer A.' These were used for the 2-variable approach.

All samples were analyzed for TOC and TN content. The average of two determinations was used for the calculations. In turn, for each of these determinations, the analyzer averaged 2 or 3 representative measurements.

Table 4. Surfactant standard solutions.

Solution	Surfactant (ppm)
SSW	0
Standard S1	25
Standard S2	50
Standard S3	75
Standard S4	100
Standard S5	150
Standard S6	200

Table 5. Polymer standard solutions.

Solution	Polymer (ppm)
SSW	0
Standard P1	10
Standard P2	25
Standard P3	50
Standard P4	75
Standard P5	100
Standard P6	150
Standard P7	200

Table 6. Surfactant-polymer standard solutions.

Solution	Surfactant (ppm)	Polymer (ppm)
Standard SP1	25	10
Standard SP2	25	200
Standard SP3	50	100
Standard SP4	100	50
Standard SP5	100	150
Standard SP6	150	100
Standard SP7	200	10
Standard SP8	200	200

## Results

### Single-variable calibration curves

The results obtained by analyzing samples shown in Table 4 and Table 5 allowed to obtain calibration curves for surfactants A and B, and for polymers A and B, respectively. The linear fit equations obtained by single-variable regression are shown in Table 7 and plotted in Figure 16, Figure 17, Figure 18, and Figure 19.

A good correlation between TOC and surfactant concentration can be observed and excellent linear-fit curves were obtained by regression. The same can be said about the correlation between TOC or TN and polymer concentration. The calibration curves are valid in the range from 0 to 200 ppm.

Table 7. Calibration curves obtained by single-variable linear regression.

Product	Equation	R <sup>2</sup>
Surfactant A	$TOC_S = 0.7776 [S] + 0.5924$	0.9996
Surfactant B	$TOC_S = 0.9137 [S] + 5.4833$	0.9954
Polymer A	$TOC_P = 0.4234 [P] + 2.1272$	0.9994
	$TN = 0.1450 [P] + 0.2254$	0.9995
Polymer B	$TOC_P = 0.4341 [P] + 1.9920$	0.9996
	$TN = 0.1445 [P] + 0.1906$	0.9996

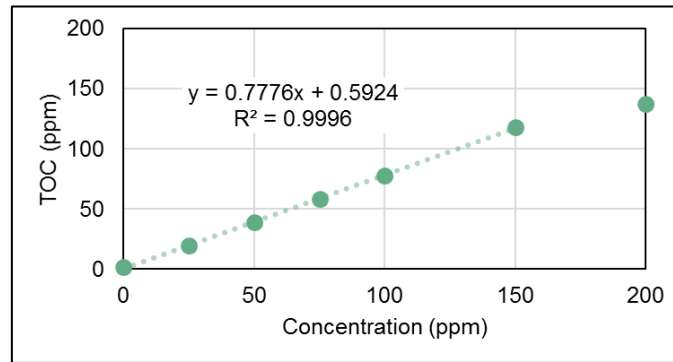


Figure 16. Surfactant A calibration curve obtained by single-variable linear regression.

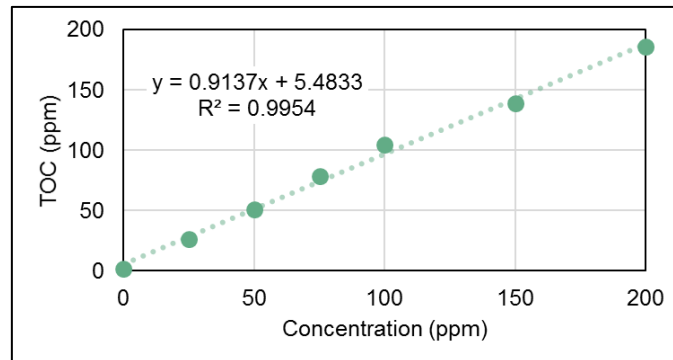


Figure 17. Surfactant B calibration curve obtained by single-variable linear regression.

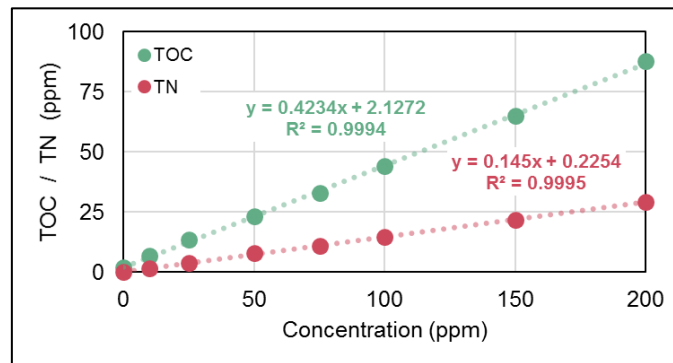


Figure 18. Polymer A calibration curves obtained by single-variable linear regression.

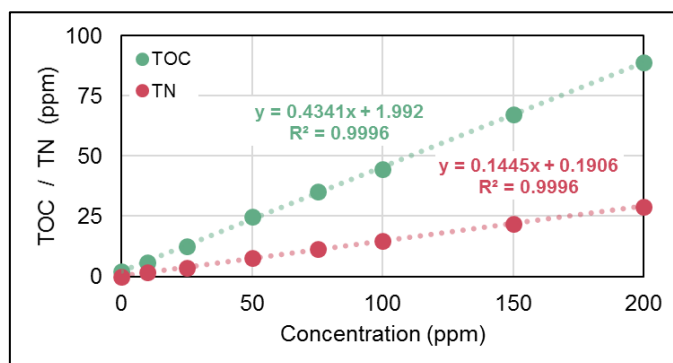


Figure 19. Polymer B calibration curves obtained by single-variable linear regression.

### 2-variable calibration curves

Three combinations of polymer and surfactant were studied by the 2-variable regression approach:

- Surfactant A + Polymer A
- Surfactant A + Polymer B
- Surfactant B + Polymer A

For each case, all samples shown in Table 4, Table 5, and Table 6 were analyzed to build calibration curves. The linear fit equations obtained by 2-variable regression are shown in Table 8.

A good correlation between TOC/TN and surfactant and polymer concentration was found and excellent linear-fit curves were obtained by regression. The calibration curves are valid in the range from 0 to 200 ppm.

Table 8. Calibration curves obtained by 2-variable linear regression.

Products	Equation	R <sup>2</sup>
Surfactant A + Polymer A	$TN = 0.1491 [P] + 0.0393$	0.9983
	$TOC = 0.7168 [S] + 0.4140 [P] + 3.9708$	0.9950
Surfactant A + Polymer B	$TN = 0.1469 [P] + 0.0161$	0.9996
	$TOC = 0.7032 [S] + 0.4121 [P] + 4.1849$	0.9937
Surfactant B + Polymer A	$TN = 0.1462 [P] + 0.1221$	0.9997
	$TOC = 0.9125 [S] + 0.4093 [P] + 3.6614$	0.9975

### Analysis of surfactant-polymer solutions

TOC and TN measurements of surfactant-polymer mixtures shown in Table 6 were used to determine surfactant and polymer content by the two proposed approaches (single- and 2-variable regression). The results were useful for testing the accuracy of the analytical method for simultaneous determination of surfactant and polymer.

For the pair Surfactant A + Polymer A, Table 9 and Figure 20 show a comparison of the real concentrations of each solution and the ones determined by TOC/TN. It can be seen that the error in surfactant determination is much higher than the error in polymer determination. This is due to



the fact that both calculation approaches propagate the error of polymer determination to surfactant determination (see Figure 14 and Figure 15). Regarding the comparison of calculation approaches, error was reduced by around 50% when using 2-variable regression. Hence, it is well worth analyzing more standard samples in order to apply this approach.

Similar results were observed for the pairs Surfactant A + Polymer B (Table 10 and Figure 21) and Surfactant B + Polymer A (Table 11 and Figure 22).

Table 9. Simultaneous determination of Surfactant A and Polymer A.

Calculation approach	Surfactant A (ppm)			Polymer A (ppm)		
	Real	Measured	Error	Real	Measured	Error
Single-variable regression	25	22.9	-2.1	10	13.5	3.5
	25	25.0	0.0	200	213.3	13.3
	50	51.3	1.3	100	100.8	0.8
	100	103.2	3.2	50	52.2	2.2
	100	82.8	-17.2	150	148.3	-1.7
	150	129.8	-20.2	100	100.2	0.2
	200	182.8	-17.2	10	10.2	0.2
	200	177.9	-22.1	200	208.6	8.6
2-variable regression	25	22.8	-2.2	10	14.3	4.3
	25	30.8	5.8	200	208.8	8.8
	50	56.0	6.0	100	99.3	-0.7
	100	110.9	10.9	50	52.1	2.1
	100	91.6	-8.4	150	145.5	-4.5
	150	141.2	-8.8	100	98.8	-1.2
	200	196.1	-3.9	10	11.2	1.2
	200	196.5	-3.5	200	204.2	4.2

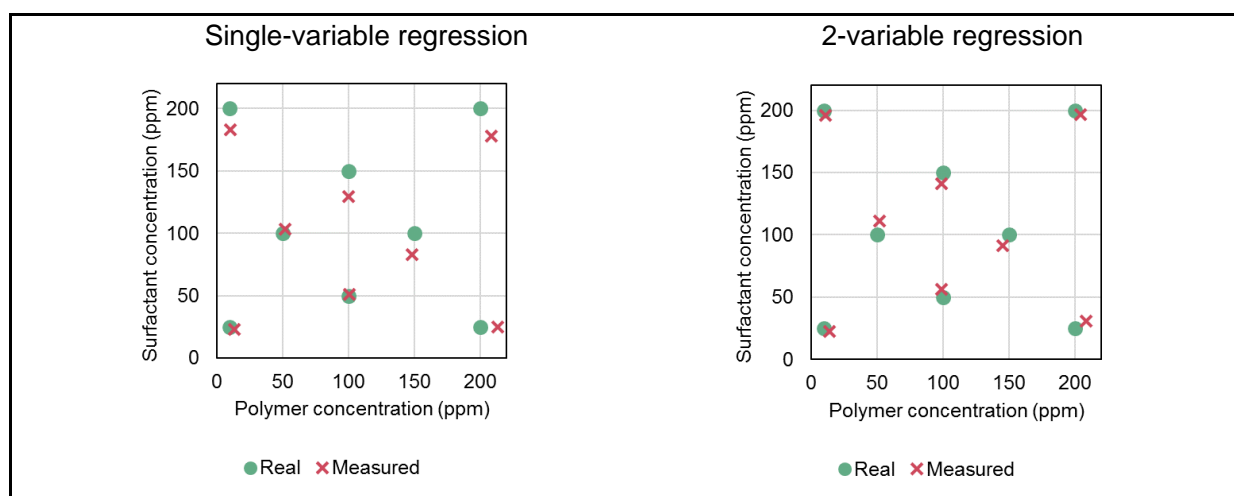


Figure 20. Simultaneous determination of Surfactant A and Polymer A.

Table 10. Simultaneous determination of Surfactant A and Polymer B.

Calculation approach	Surfactant A (ppm)			Polymer B (ppm)		
	Real	Measured	Error	Real	Measured	Error
Single-variable regression	25	22.2	-2.8	10	10.5	0.5
	25	25.0	0.0	200	203.8	3.8
	100	106.8	6.8	50	49.5	-0.5
	100	75.6	-24.4	150	152.4	2.4
	150	125.9	-24.1	100	99.3	-0.7
	200	176.9	-23.1	10	11.6	1.6
	200	172.8	-27.2	200	205.4	5.4
2-variable regression	25	22.0	-3.0	10	11.5	1.5
	25	33.0	8.0	200	201.8	1.8
	100	117.1	17.1	50	49.9	-0.1
	100	86.8	-13.2	150	151.2	1.2
	150	140.2	-9.8	100	99.0	-1.0
	200	193.2	-6.8	10	12.6	2.6
	200	196.4	-3.6	200	203.3	3.3

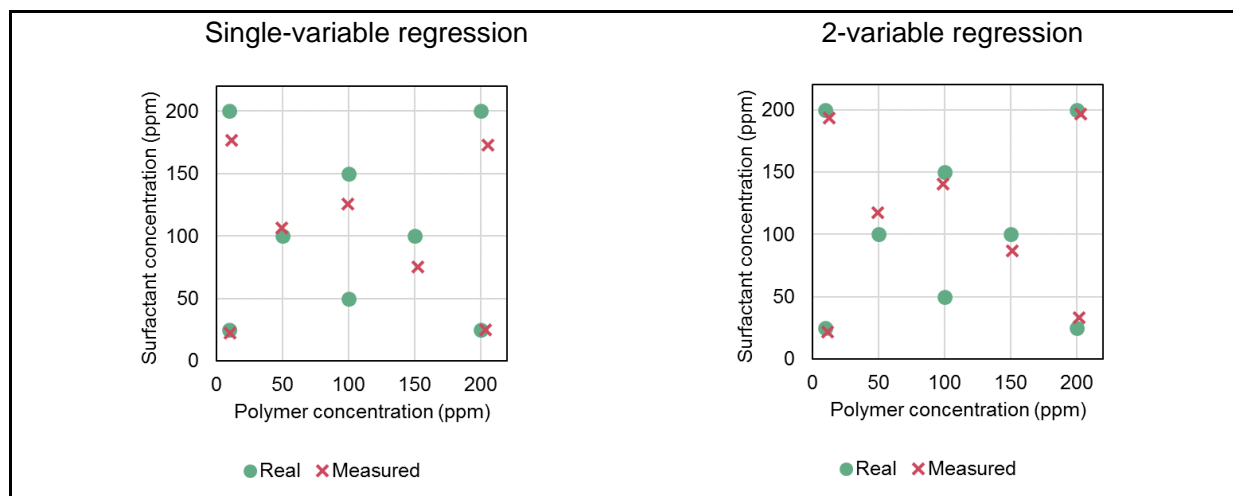


Figure 21. Simultaneous determination of Surfactant A and Polymer B.

Table 11. Simultaneous determination of Surfactant B and Polymer A.

Calculation approach	Surfactant B (ppm)			Polymer A (ppm)		
	Real	Measured	Error	Real	Measured	Error
Single-variable regression	25	20.7	-4.3	10	11.1	1.1
	100	86.9	-13.1	50	48.2	-1.8
	100	88.8	-11.2	150	150.0	0.0
	150	143.7	-6.3	100	98.7	-1.3
	200	191.6	-8.4	10	8.3	-1.7
	200	196.4	-3.6	200	201.7	1.7
2-variable regression	25	24.9	-0.1	10	11.8	1.8
	100	92.0	-8.0	50	48.5	-1.5
	100	95.8	-4.2	150	149.5	-0.5
	150	149.8	-0.2	100	98.7	-1.3
	200	196.1	-3.9	10	9.0	-1.0
	200	204.6	4.6	200	200.8	0.8

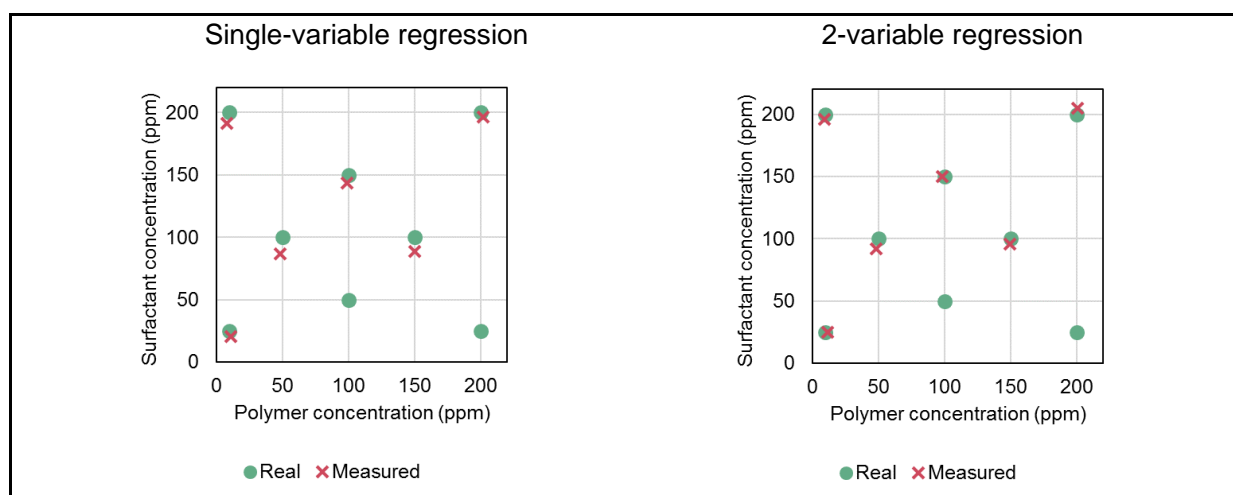


Figure 22. Simultaneous determination of Surfactant B and Polymer A.

## Conclusions

- Polymers can be determined by either TOC or TN content, while surfactants can be determined by TOC content. Excellent calibration curves could be obtained by single-variable linear regression in the range from 0 to 200 ppm.
- Surfactant and polymer can be determined in mixtures by simultaneous measurement of TOC and TN, given only the polymer contains nitrogen. Two approaches are possible for calculation, based on single- and 2-variable linear regression. The 2-variable-regression approach requires the analysis of more standard samples to obtain calibration curves but the error is reduced approximately 50% compared to the single-variable approach. Excellent calibration curves could be obtained in the range from 0 to 200 ppm.
- When analyzing surfactant-polymer mixtures by TOC and TN, error in surfactant determination is higher than in polymer due to the calculation scheme, which propagates error to surfactant concentration.



# DETERMINATION OF SURFACTANT AND POLYMER RETENTION

## Determination of surfactant and polymer adsorption in static conditions

### *Introduction*

Adsorption of surfactant and polymer, both individually and mixed, was studied in Bentheimer sand in static conditions. This kind of experiment does not provide realistic values for retention in dynamic conditions in the reservoir, with results usually being much higher. However, they are a good way to understand how surfactants and polymers are adsorbed and to determine maximum boundaries for adsorption.

The following objectives were established:

- Determination of surfactant and polymer adsorption isotherms
- Test the suitability of TOC-TN analysis for surfactant and polymer concentration determination in adsorption experiments

### *Materials*

Surfactant:

- Surfactant A (sulfate)

Polymer:

- Polymer A (HPAM)

Brine:

- Synthetic sea water (SSW), with composition detailed in Table 3.

Solid adsorbent:

- Crushed Bentheimer sandstone, with particle size in the range from 63 to 315  $\mu\text{m}$ . The sand was cleaned with deionized water and dried in oven at 75°C overnight, in order to remove fines.

### *Methodology*

#### *Adsorbate solution preparation*

Solutions described in Table 12, Table 13, and Table 14 were prepared for the static adsorption study of surfactant, polymer, and surfactant-polymer, respectively. All samples were prepared in synthetic sea water.

Table 12. Surfactant solutions for static adsorption test.

Solution	Surfactant (ppm)
SSW	0
S1	50
S2	100
S3	200
S4	300
S5	500
S6	1000
S7	1250
S8	1500
S9	1750
S10	2000

Table 13. Polymer solutions for static adsorption test.

Solution	Polymer (ppm)
SSW	0
P1	50
P2	100
P3	200
P4	300
P5	500
P6	1000
P7	1500

Table 14. Surfactant-polymer solutions for static adsorption test.

Solution	Surfactant (ppm)	Polymer (ppm)
P7	0	1500
SP1	50	1500
SP2	100	1500
SP3	200	1500
SP4	500	1500
SP5	1000	1500
SP6	1500	1500

### **Static adsorption experiment**

The following procedure was applied to each adsorbate solution in order to allow adsorption onto sand until equilibrium:

1. 40 g of adsorbate solution were placed in a 50-mL bottle.
2. 20 g of sand were added.
3. The bottle was hermetically sealed in order to avoid sample loss.
4. The bottle was shaken to ensure good contact between solid particles and liquid phase.
5. The bottle was left at 23°C during 4 days, in horizontal position, so that the solid was as extended as possible. A roller mixer was used to favor contact between phases. A gentle mixing was done by setting a low rotation speed with 15 rpm.

### **Sample analysis**

After solid and liquid phases had been in contact for 4 days, analyses were done to determine surfactant and polymer equilibrium concentration:

1. Supernatant liquid was separated from solid.
  - a. Surfactant samples were filtered through 1- $\mu$ m PTFE membranes.
  - b. Polymer and surfactant-polymer samples were centrifuged.
2. Samples were diluted with SSW. This was done in order to have enough volume for the TOC-TN analyzer, to ensure that the samples were within the concentration range of the calibration curves, and to reduce the viscosity, as required by the autosampler.
3. Diluted samples were analyzed for TOC and TN content.
4. Surfactant/polymer concentration was calculated by using previously determined calibration curves. The calibration curve equations obtained by linear regression are shown in Table 7 and Table 8. They are valid in the range from 0 to 200 ppm.
5. For surfactant-alone and polymer-alone solutions, single-variable calibration curves were used. On the other hand, the 2-variable-regression approach was preferred for surfactant-polymer mixture.

### **Results**

Figure 23 shows how the static adsorption experiment was carried out. One of the bottles can be seen on the left and a set of bottles in the roller mixer can be seen in the photograph on the right.



*Figure 23. Static adsorption experiment.*

After reaching equilibrium, surfactant/polymer concentration in the liquid was analyzed. By material balance between initial and final equilibrium concentration,  $C_0$  and  $C_e$ , adsorption per unit mass of sand was calculated:

$$\Gamma = \frac{m_l \times (C_0 - C_e)}{m_s} \quad (7)$$

where  $m_l$  is the mass of liquid solution and  $m_s$  is the mass of sand in the bottle.

### Surfactant

Figure 24 shows the results obtained for Surfactant A. The isotherm has two plateaus, with 105 and 760  $\mu\text{g/g}$  of adsorption, and the inflection point being close to 1000 ppm. This kind of behavior was explained by Kwok et al [21] for non-ionic surfactants (Figure 25). According to their model, a first layer of surfactant is adsorbed on the solid surface, reaching the first plateau. Then, these adsorbed molecules can favor the adsorption of a second surfactant layer by hydrophobic interaction, reaching the second plateau. However, Surfactant A is anionic (sulfate) and an isotherm with only one plateau was expected. The observed behavior could have been caused by the presence of other substances in Surfactant A formulation, which could have been adsorbed in a first layer and could have generated hydrophobic interactions to adsorb a second layer of sulfate, thus generating the second plateau.

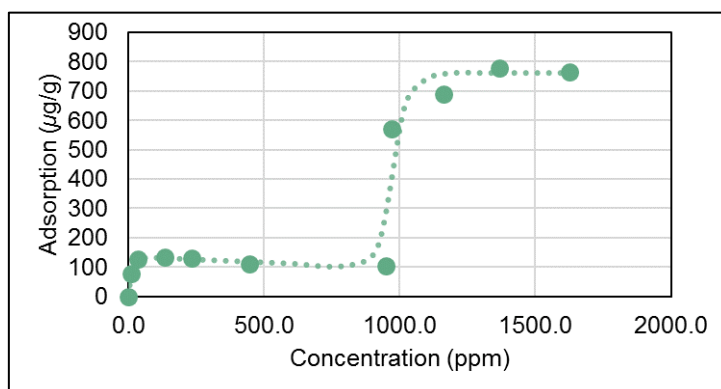


Figure 24. Surfactant A adsorption isotherm at 23°C.



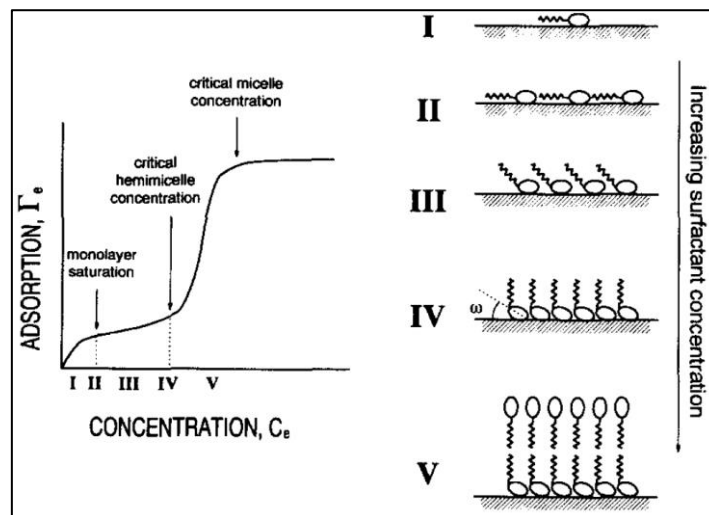


Figure 25. Adsorption isotherm and model for the adsorption of non-ionic surfactant, showing the orientation of surfactant molecules at the surface [21].

**Polymer**

Figure 26 is a plot for Polymer A adsorption isotherm. A Langmuir-type behavior was observed until 1000 ppm, with a maximum adsorption of 102  $\mu\text{g/g}$ . One point with very high adsorption, 426  $\mu\text{g/g}$ , was observed at 1289 ppm. It is recommended to do more experiments, at higher polymer concentration, to elucidate whether this last point was an error or the polymer behaved similarly to surfactant, with multilayer adsorption.

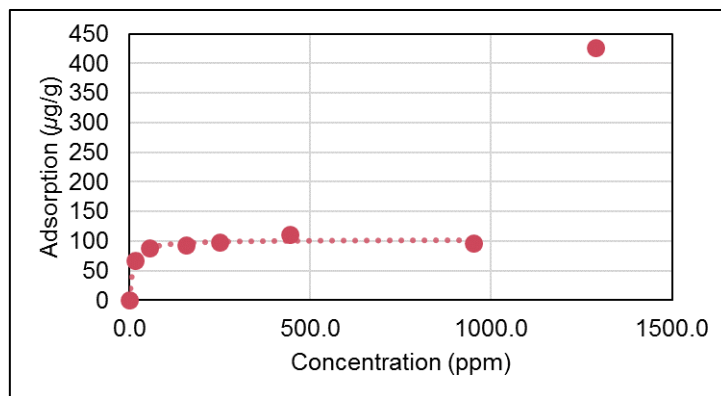


Figure 26. Polymer A adsorption isotherm at 23°C.

**Surfactant + polymer**

Figure 27 shows the adsorption isotherms obtained for Surfactant A with and without 1500 ppm of Polymer A. At surfactant concentration below 950 ppm, surfactant adsorption reached 157  $\mu\text{g/g}$  when polymer was present, i.e. adsorption was 50% higher. This could be a consequence of adsorbed polymer molecules providing new adsorption sites for surfactant. On the other hand, above 1000 ppm of surfactant, polymer prevented the adsorption of the second surfactant layer, hence reducing surfactant adsorption by 80%.

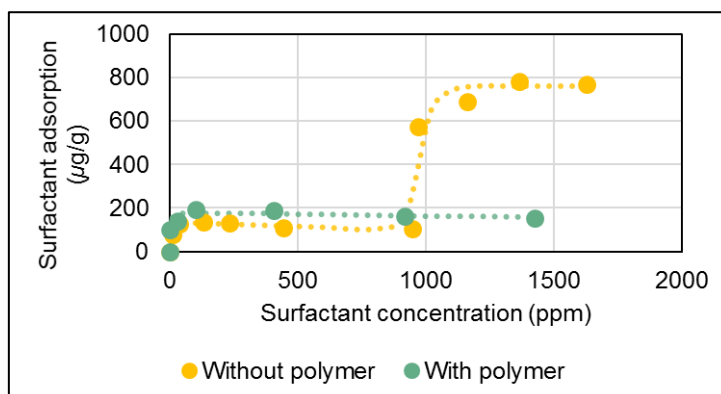


Figure 27. Surfactant A adsorption isotherm at 23°C, with and without polymer.

Figure 28 shows polymer adsorption as a function of surfactant concentration in red and surfactant adsorption in green, being polymer initial concentration always 1500 ppm. At low surfactant concentration, there was a competition for adsorption sites and surfactant was preferably adsorbed by sand. Therefore, polymer adsorption was reduced by 85%, reaching 54 µg/g. As surfactant concentration was increased above 200 ppm, polymer adsorption increased until 173 µg/g, possibly by adsorption of a new layer. Nevertheless, final polymer adsorption was reduced by 60% due to surfactant presence.

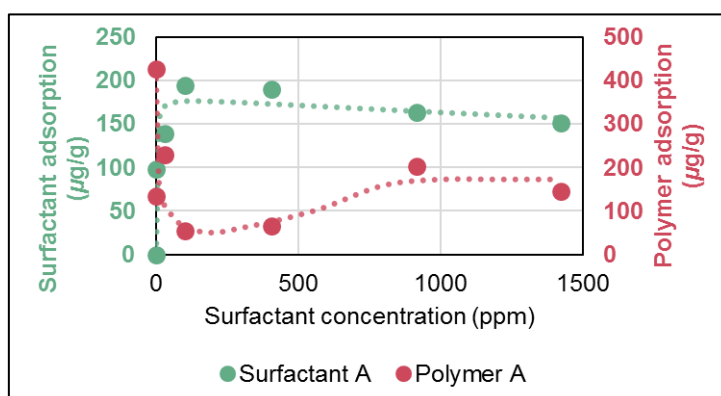


Figure 28. Simultaneous adsorption of Surfactant A and Polymer A at 23°C.

## Conclusions

- Adsorption isotherms were obtained and maximum adsorption values were determined, as shown in Table 15. In general, it can be said that competitive adsorption can reduce both surfactant and polymer retention.
- Multilayer adsorption was observed for Surfactant A. The adsorption of the second layer was prevented by the presence of polymer and this reduced surfactant adsorption by 80%.
- Polymer A may also have a multilayer adsorption behavior. It is recommended to do further experiments to verify this.
- TOC and TN analysis are suitable for surfactant and polymer concentration determination in static adsorption experiments.

Table 15. Maximum adsorption values observed at 23°C.

Chemical	Maximum adsorption ( $\mu\text{g/g}$ )	
	Surfactant A	105 [S] < 1000 ppm
Polymer A	102 [P] < 1000 ppm	426* [P] > 1000 ppm
Surfactant A in presence of Polymer A	157	
Polymer A in presence of Surfactant A	173	
*More experiments are needed to vary this value.		

## Determination of surfactant and polymer retention in dynamic conditions

### Introduction

Retention of surfactant and polymer, both individually and mixed, was studied in a Bentheimer sandpack under flow conditions. The following objectives were established:

- Determination of dynamic retention of surfactant and polymer:
  - In steady-state flow at a concentration of 1500 ppm
  - Residual retention after water flooding
- Determination of sandpack properties:
  - Permeability
  - Porosity
- Test the suitability of TOC-TN analysis for surfactant and polymer concentration determination in effluents

### Materials

Surfactant solution:

- Surfactant A, 1500 ppm, prepared in SSW brine, filtered through 1.2- $\mu\text{m}$  membrane.

Polymer solution:

- Polymer A, 1500 ppm, prepared in SSW brine, filtered through 1.2- $\mu\text{m}$  membrane.

Brine:

- Synthetic sea water (SSW), with composition detailed in Table 3.

Solid adsorbent:

- Crushed Bentheimer sandstone, with particle size in the range from 63 to 315  $\mu\text{m}$ . The sand was cleaned with deionized water and dried in oven at 75°C overnight, in order to remove fines. Then, it was packed in a column which was used as porous media. A new clean column was used for each studied solution.

## Methodology

### Sandpack assembly

#### Dead volume determination

Before setting up the sandpack, the dead volume,  $V_d$ , was determined. This is the volume of all parts of the system, excluding the sand column, i.e. the volume of tubes, couplings and fittings. It was determined as follows:

1. Column was bypassed and the whole system was dried.
2. Brine was injected at a known constant flowrate.
3. Time was accounted until the first drop of liquid came out of the system. This is the time required to displace all air in the system and fill dead space with brine.
4. Dead volume was determined by multiplying flowrate and time.

#### Sandpack setup and pore volume determination

The sand was wet packed in the column and pore volume,  $V_p$ , was determined by the following procedure:

1. A known volume of brine was injected into the bottom of the empty column.
2. A known mass of dry sand was poured into the column through the open top. As a result, sand settled in the bottom and brine was displaced. A fraction of the brine remained in the pore space between sand grains, while the rest was on top of the sand layer. Brine on top of the sand layer was extracted and its volume was determined.
3. Pore volume was calculated by subtracting extracted-brine volume from the initial volume that had been injected before adding sand.
4. The column was tightly capped on the top.
5. Brine was injected from bottom to top of the column, until pressure stabilized. It was checked that no air bubbles were visible.

### Permeability determination

Sandpack permeability to brine was determined by flowrate variation and differential pressure measurement between sandpack inlet and outlet.

1. Brine was injected upwards through the column at known flowrate until pressure stabilized. Differential pressure between inlet and outlet was measured. This was done for the following flowrates: 0.2, 0.5, 1.0, and 1.5 mL/min.
2. Considering Darcy's law, permeability was determined by least-squares linear regression of pressure drop as a function of flowrate:

$$\Delta P = \frac{\mu L}{k A} q + (\rho g L + P_{\text{loss}}) \quad (8)$$

Permeability was determined from the slope of the line. The intercept is a combination of liquid column head and other pressure losses that could have occurred in the system.

### Dynamic retention experiment

After permeability determination, the sandpack was stabilized at a flowrate of 0.2 mL/min by brine injection. Then, the following injection scheme was followed in order to determine surfactant/polymer retention in the sandpack:

1. Surfactant/polymer solution was injected upwards through the column at a flowrate of 0.2 mL/min. A sufficient amount was injected in order to ensure the effluent reached injected surfactant/polymer concentration.

2. Brine was injected until no more surfactant/polymer was detected in the effluent, at a flowrate of 0.2 mL/min.

The experiment was carried out at a temperature of 23°C.

### ***Effluent sample collection and analysis***

During the dynamic retention experiment, 4-mL effluent samples were collected for surfactant/polymer concentration determination by TOC and TN:

1. 3 mL of each sample were diluted to 50 mL. This was done in order to have enough volume for the TOC-TN analyzer, to ensure that the sample was within the concentration range of the calibration curves, and to reduce the viscosity, as required by the autosampler.
2. Diluted samples were analyzed for TOC and TN content.
3. Surfactant/polymer concentration was calculated by using previously determined calibration curves. The calibration curve equations obtained by linear regression are shown in Table 7. They are valid in the range from 0 to 200 ppm.

## **Results**

### ***Sandpack properties***

Photographs of the system for determination of dynamic retention in a sandpack are shown in Figure 29. From right to left, injection fluid bottle, pumping system, pressure gauge, sandpack column, and sample collector can be seen. Table 16 shows the characteristics of the sandpack columns used for each studied EOR chemical.



Figure 29. Sandpack equipment.

Table 16. Sandpack properties.

Property	Sandpack	Surfactant A	Polymer A
Sand content, $m_s$ (g)		136.05	136.61
Column height, $L$ (cm)		19.00	19.00
Column diameter, $D$ (cm)		2.80	2.80
Cross section area, $A$ (cm <sup>2</sup> )		6.16	6.16
Bulk volume, $V_b$ (cm <sup>3</sup> )		116.99	116.99
Dead volume, $V_d$ (cm <sup>3</sup> )		5.02	5.02
Pore volume, $V_p$ (cm <sup>3</sup> )		41.10	40.50
Porosity, $\phi$ (%)		35.13	34.62
Permeability, $k$ (D)		11.23	9.65

Permeability was determined by flowrate variation. Figure 30 and Figure 31 show the linear regression equations obtained for pressure drop versus flowrate in SI units. The slope of the line allows for permeability calculation according to Equation 8. A brine viscosity of 1 cP was used for the calculations.

The values obtained for porosity and permeability are in good agreement with values published in literature for very-well-sorted medium- to fine-grain unconsolidated sand [9].

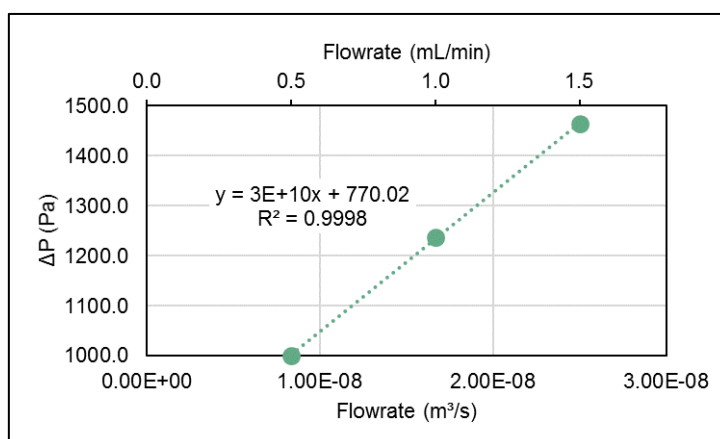


Figure 30. Permeability determination by flowrate variation for Surfactant A sandpack.

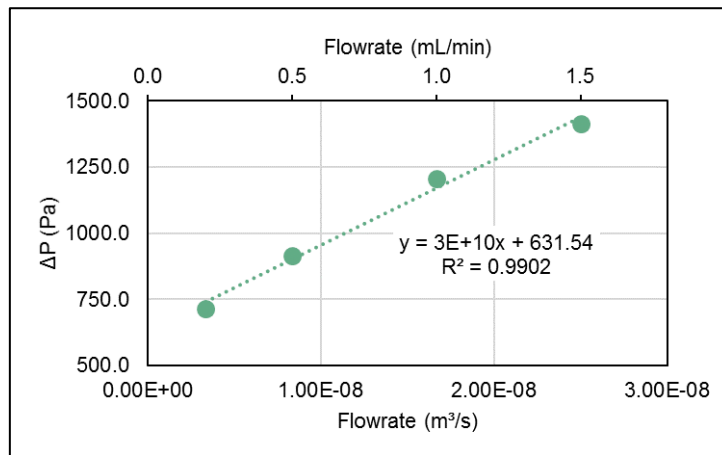


Figure 31. Permeability determination by flowrate variation for Polymer A sandpack.

**Dynamic retention of Surfactant A**

Figure 32 shows the results obtained for the dynamic retention experiment of Surfactant A. Normalized concentration of surfactant is plotted against fluid volume, expressed as pore volume multiplier (PV). The red curve is injected fluid concentration, which is 1500 ppm until 5.84 PV (surfactant injection) and then falls to zero (brine injection). On the other hand, the green dots represent the concentration determined in the effluent.

Surfactant breakthrough was observed at 1.17 PV and concentration increased abruptly until reaching injected concentration, which means the flow was very close to piston-like behavior. Similar behavior was observed after the beginning of brine injection, with an abrupt fall in effluent concentration.

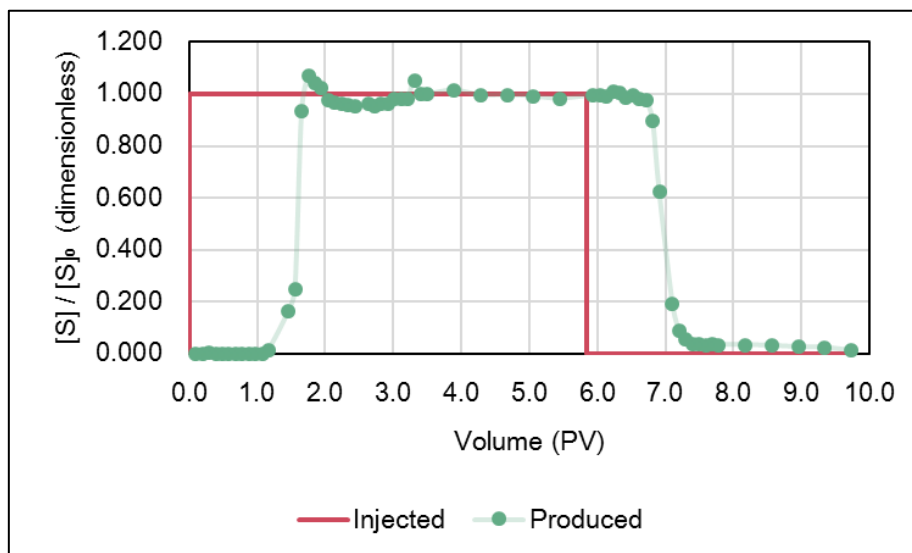


Figure 32. Normalized injected and produced concentrations of Surfactant A during dynamic retention experiment.

In order to calculate the cumulative mass of produced surfactant, the effluent concentration curve was integrated numerically by using the trapezoidal rule:

$$[[S]]_p = [S]_0 \times \int_0^{V_n} \frac{[S]}{[S]_0} dV \approx [S]_0 \times \sum_{j=1}^n (V_j - V_{j-1}) \left( \frac{[S]_j + [S]_{j-1}}{2} \right) \quad (9)$$

Similarly, the cumulative mass of injected surfactant was calculated:

$$[[S]]_i = [S] \times V \quad (10)$$

Figure 33 shows cumulative mass of injected and produced surfactant. The difference between these two values,  $[[S]]_i - [[S]]_p$ , is the amount of surfactant that remained inside the system at each moment (Figure 34). This amount is the sum of the following contributions:

- Surfactant retained in sandpack
- Free surfactant in the solution contained in pore volume
- Free surfactant in the solution contained in dead volume

Since pore volume and dead volume are known, the amount of surfactant retained in the sandpack can be calculated.

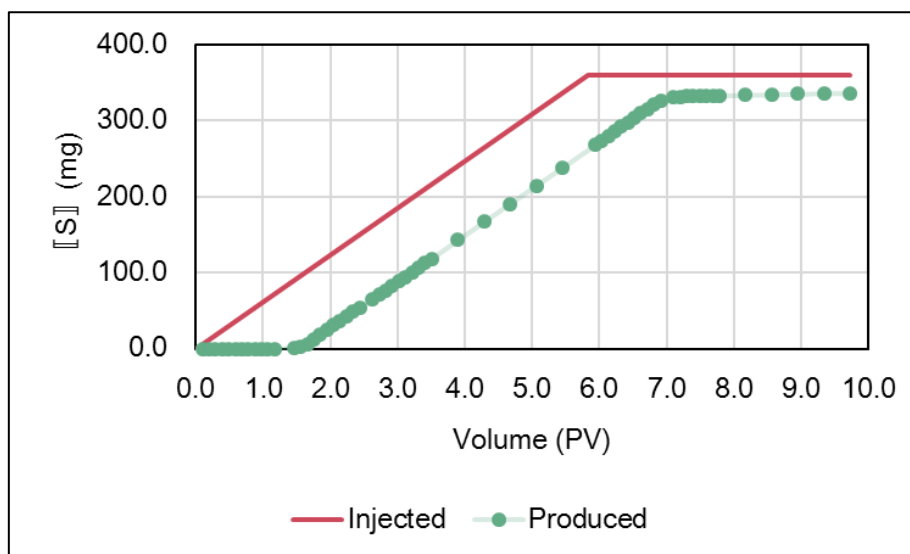


Figure 33. Cumulative mass of injected and produced Surfactant A during dynamic retention experiment.



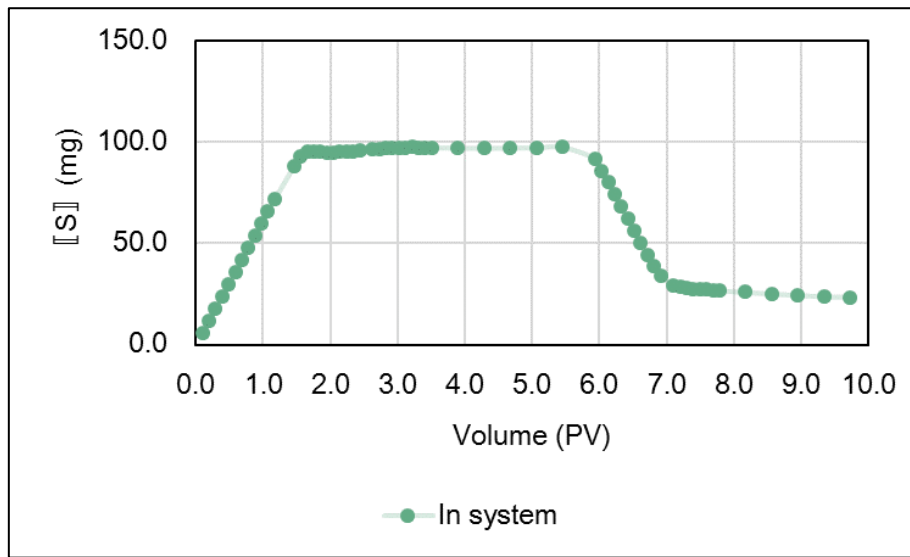


Figure 34. Cumulative mass of Surfactant A that remained inside the system during dynamic retention experiment.

#### Dynamic surfactant retention in steady state

As seen in Figure 34, cumulative surfactant mass inside the system increased linearly before surfactant breakthrough. This is due to the fact that surfactant was injected at constant concentration and rate. After breakthrough, accumulation speed decreased rapidly and a plateau was reached with 97 mg of surfactant accumulated in the system. Upon reaching this plateau, produced concentration equaled injected concentration and no further accumulation occurred. In this situation, the whole system contained surfactant solution at the injected concentration,  $[S]_0 = 1500$  ppm. Hence, surfactant retention at this concentration, in this steady state condition, could be calculated by mass balance:

$$\Gamma_s = \frac{[S]_i - [S]_p - [S]_0 \times V_p - [S]_0 \times V_d}{m_s} \quad (11)$$

Note that it was divided by sand mass,  $m_s$ , in order to obtain surfactant mass retained per unit mass of adsorbent.

Surfactant retention was found to be  $206 \mu\text{g/g}$  (Table 17). This is the maximum amount of surfactant that the sandpack can retain in these flow conditions and at a concentration of 1500 ppm. It represents 7.8% of total injected surfactant and only 27% of the amount adsorbed in static conditions.

#### Residual surfactant retention

After injecting 5.84 PV of surfactant, water flooding began. As the system was flushed by brine, surfactant mass accumulation decreased (Figure 34) by drainage of pore and dead volume and by surfactant desorption. A new plateau was reached with 24 mg of surfactant accumulated in the system. Upon reaching this plateau, no surfactant was detected in the effluent. In this situation, the whole system was filled with brine and the only accumulated surfactant was the residual surfactant which was irreversibly retained by the sandpack. The residual retention was calculated by material balance:

$$\Gamma_s = \frac{[S]_i - [S]_p}{m_s} \tag{12}$$

Residual surfactant retention after water flooding was found to be 172  $\mu\text{g/g}$  (Table 17). This represents 6.5% of total injected surfactant. Only 16.4% of the originally retained surfactant was desorbed by water flooding, which indicates surfactant retention by sandpack is practically irreversible.

Table 17. Dynamic retention of Surfactant A in sandpack at 23°C.

Retention in steady state at $[S] = 1500 \text{ ppm } (\mu\text{g/g})$	206
Residual retention after water flooding ( $\mu\text{g/g}$ )	172

**Dynamic retention of Polymer A**

Figure 35 shows the results obtained for the dynamic retention experiment of Polymer A. Normalized polymer concentration is plotted against fluid volume, expressed as pore volume multiplier (PV). The red curve is the concentration of injected fluid, which is 1500 ppm until 7.9 PV (polymer injection) and then falls to zero (brine injection). On the other hand, the green dots represent the concentration determined in the effluent.

Polymer breakthrough was observed at 1.19 PV and concentration increased abruptly until reaching injected concentration, which means the flow was very close to piston-like behavior. After the beginning of brine injection, the fall in effluent concentration was not that abrupt. This could be due to the fact that brine is less viscous than polymer (1 cP vs 14.2 cP) thus being less efficient to push polymer solution. Besides, polymer desorption might have occurred at a low speed.

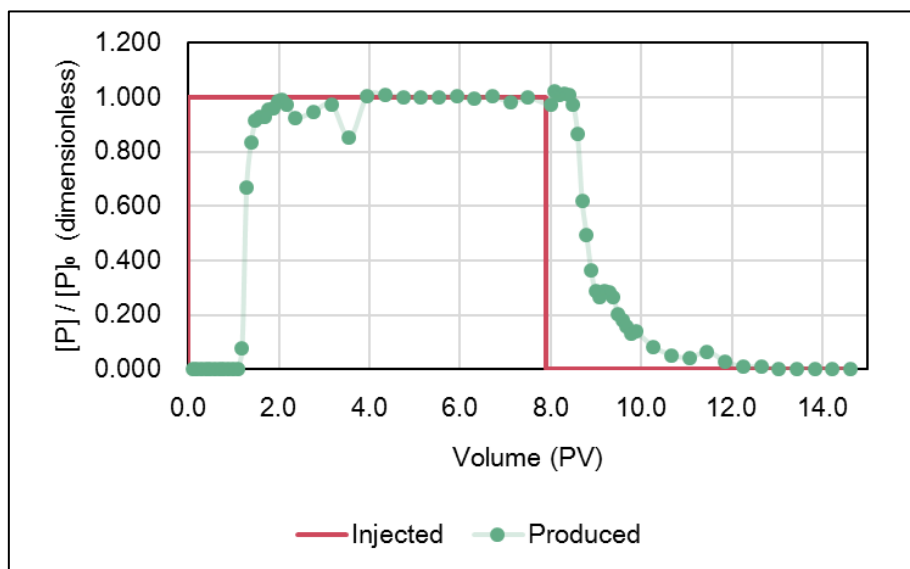


Figure 35. Normalized injected and produced concentrations of Polymer A during dynamic retention experiment.

In order to calculate the cumulative mass of produced polymer, the effluent concentration curve was integrated numerically by using the trapezoidal rule:

$$[[P]]_p = [P]_0 \times \int_0^{V_n} \frac{[P]}{[P]_0} dV \approx [P]_0 \times \sum_{j=0}^n (V_j - V_{j-1}) \left( \frac{[P]_j + [P]_{j-1}}{2} \right) \quad (13)$$

Similarly, the cumulative mass of injected polymer was calculated:

$$[[P]]_i = [P] \times V \quad (14)$$

Figure 36 shows cumulative mass of injected and produced polymer. The difference between these two values,  $[[P]]_i - [[P]]_p$ , is the amount of polymer that remained inside the system at each moment (Figure 37). This amount is the sum of the following contributions:

- Polymer retained in sandpack
- Free polymer in the solution contained in pore volume
- Free polymer in the solution contained in dead volume

Since pore volume and dead volume are known, the amount of polymer retained in the sandpack can be calculated.

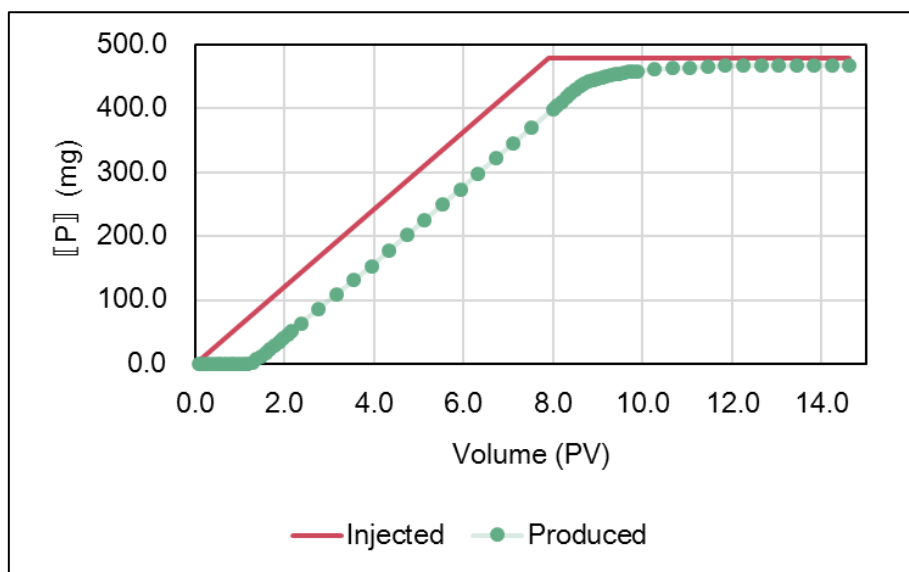


Figure 36. Cumulative mass of injected and produced Polymer A during dynamic retention experiment.

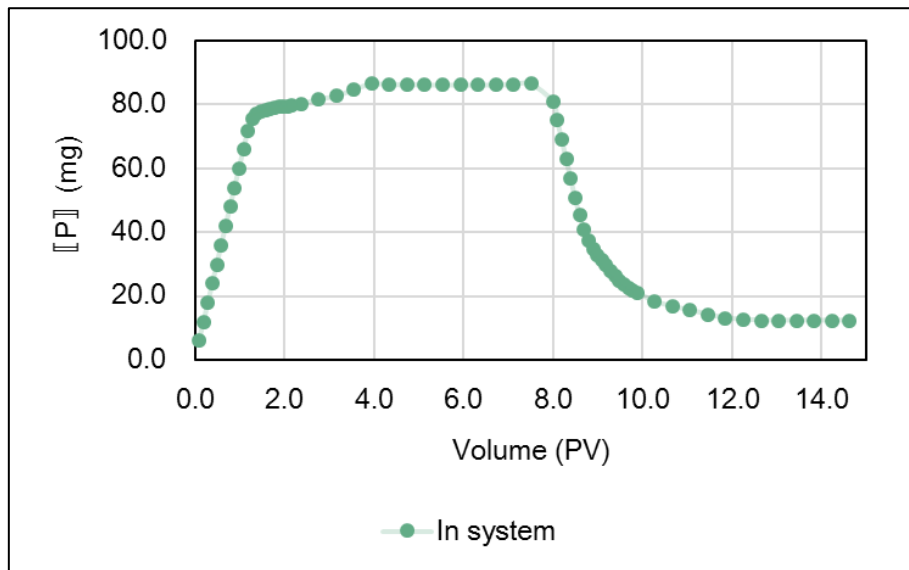


Figure 37. Cumulative mass of Polymer A that remained inside the system during dynamic retention experiment.

#### Dynamic polymer retention in steady state

As seen in Figure 37, cumulative polymer mass inside the system increased linearly before polymer breakthrough. This is due to the fact that polymer was injected at constant concentration and constant rate. After breakthrough, accumulation speed decreased rapidly and a plateau was reached with 86 mg of polymer accumulated in the system. Upon reaching this plateau, produced concentration equaled injected concentration and no further accumulation occurred. In this situation, the whole system contained polymer solution at the injected concentration,  $[P]_0 = 1500$  ppm. Hence, polymer retention at this concentration, in this steady state condition, could be calculated by mass balance:

$$\Gamma_p = \frac{[P]_i - [P]_p - [P]_0 \times V_p - [P]_0 \times V_d}{m_s} \quad (15)$$

Note that it was divided by sand mass,  $m_s$ , in order to obtain polymer mass retained by unit mass of adsorbent.

Polymer retention was found to be  $132 \mu\text{g/g}$  (Table 18). This is the maximum amount of polymer that the sandpack can retain in these flow conditions and at a concentration of 1500 ppm. It represents 3.8% of total injected polymer and only 31% of the amount adsorbed in static conditions.

#### Residual polymer retention

After injecting 7.9 PV of polymer, water flooding began. As the system was flushed by brine, polymer mass accumulation decreased (Figure 37) by drainage of pore and dead volume and by polymer desorption. A new plateau was reached with 12 mg of polymer accumulated in the system. Upon reaching this plateau, no polymer was detected in the effluent. In this situation, the whole system was filled with brine and the only accumulated polymer was the residual polymer which was irreversibly retained by the sandpack. The residual retention was calculated by material balance:

$$\Gamma_p = \frac{[[P]]_i - [[P]]_p}{m_s} \quad (16)$$

Residual polymer retention after water flooding was found to be 90  $\mu\text{g/g}$  (Table 18). This represents 2.6% of total injected polymer. An amount of 31.7% of the originally retained polymer was desorbed by water flooding, which indicates polymer retention by sandpack is mostly irreversible, though not completely.

Table 18. Dynamic retention of Polymer A in sandpack at 23°C.

Retention in steady state at $[P] = 1500 \text{ ppm } (\mu\text{g/g})$	132
Residual retention after water flooding ( $\mu\text{g/g}$ )	90

## Conclusions

- When 1500-ppm solutions of Surfactant A and Polymer A in synthetic sea water were injected into separate Bentheimer sandpacks at a flowrate of 0.2 mL/min, maximum amounts of 206 and 132  $\mu\text{g/g}$  were retained at 23°C, respectively. This is only approximately 30% of the amount adsorbed in static conditions.
- After water flooding, only 16.4% of retained surfactant was desorbed, reaching a residual retention of 172  $\mu\text{g/g}$ . Therefore, it can be said that surfactant retention is practically irreversible. On the other hand, polymer residual retention was 90  $\mu\text{g/g}$ , i.e. 31.7% of retained polymer was desorbed by water flooding. Hence, it can be said that polymer retention is mostly irreversible, though not completely.
- The surfactant concentration variation observed in the effluent showed flow was very close to piston-like behavior, with surfactant breakthrough after injection of 1.17 PV. In the polymer case, flow was very close to piston-like behavior during polymer injection in the initially brine-saturated sandpack, with polymer breakthrough after injection of 1.19 PV. However, when brine was injected in the polymer-saturated sandpack, flow behavior was not piston-like and polymer concentration decreased gradually. This is a consequence of slow polymer desorption and brine not being efficient to push polymer due to its low viscosity.
- The sandpack columns, with grain size in the range from 63 to 315  $\mu\text{m}$ , had very high permeability and porosity, as expected for well-sorted unconsolidated sand. The values were 9.7-11.2 D and 34.6-35.1%, respectively.
- TOC and TN analysis are suitable for surfactant and polymer concentration determination in sandpack and core flooding experiments.



## CONCLUSIONS

- Surfactant and polymer concentration can be determined by TOC and TN content measurement. If polymer contains nitrogen but surfactant does not, which is the usual case in EOR, mixtures can be analyzed and two approaches are possible for calculation based on single- and 2-variable linear regression. The 2-variable-regression approach requires the analysis of more standard samples to obtain calibration curves but the error is reduced approximately 50% compared to the single-variable approach.
- Many other analytical methods could be used to determine polymer and surfactant but TOC and TN analysis has the advantage of being accurate and simple to execute. One single piece of equipment can analyze both TOC and TN and an autosampler can be used for automatic measurement. This makes it very convenient for retention determination experiments and coreflood tests in which many samples need to be analyzed. However, if a formulation contains 2 or more different surfactants, HPLC is recommended, since it allows to determine each component individually, unlike TOC method which determines overall surfactant concentration.
- Adsorption isotherms were obtained for an anionic sulfate surfactant and partially hydrolyzed polyacrylamide onto Bentheimer sand in static conditions at 23°C. It was found that surfactant was adsorbed in two layers, with two plateaus in the adsorption isotherm and a maximum adsorption of 760  $\mu\text{g/g}$  above 1000 ppm. Polymer may have been adsorbed in two layers, as well, but further experiments need to be done to confirm this. Maximum observed polymer adsorption was 426  $\mu\text{g/g}$ .
- When surfactant and polymer were mixed, competitive adsorption occurred and retention values were reduced for both surfactant and polymer in static conditions. Moreover, polymer prevented the adsorption of the second surfactant layer, thus reducing its retention by 80%.
- Dynamic retention experiments were carried out in Bentheimer sandpacks with 0.2-mL/min flowrate, at 23°C. Retention at 1500 ppm was approximately 30% of that observed in static conditions, with values of 206 and 132  $\mu\text{g/g}$  for surfactant and polymer, respectively.
- After water flooding, only 16.4% of previously adsorbed surfactant was desorbed, reaching a residual retention of 172  $\mu\text{g/g}$ . Regarding polymer, 31.7% was desorbed by water flooding, with a residual retention of 90  $\mu\text{g/g}$ . It can be said that retention is largely irreversible.
- The experiments that were carried out allow to better understand the behavior of BASF products for EOR. It is recommended to continue this type of studies with other surfactants and polymers. Retention data can be used for screening, EOR process design, simulation, etc.
- Though both static and dynamic experiments allowed for retention determination, the values obtained in static conditions are extremely high and not very representative of what could be observed in the porous media. However, they are useful to understand adsorption phenomena and establish maximum boundaries of retention.
- The sandpack methodology proved useful to determine surfactant and polymer retention, with values that should be more representative of retention in reservoir rock. However, since sand is unconsolidated, the results can be different from the ones observed in core samples. When possible, it is recommended to do the experiment by core flooding rather than with a sandpack.
- In the future, the methodology to determine surfactant and polymer retention could also be applied in the field. The data obtained from pilot tests could be much more representative of reservoir behavior than the data obtained in laboratory, whether in sandpack or core flooding experiments. Moreover, the methodology could be applied for surveillance of EOR processes in the field.





## REFERENCES

- [1] H. Alhassawi and L. Romero-Zerón, "Novel Surfactant Delivery System for Controlling Surfactant Adsorption onto Solid Surfaces. Part II: Dynamic Adsorption Tests," *Canadian Journal of Chemical Engineering*, vol. 93, pp. 1371-1379, 2015.
- [2] V. Alvarado and E. Manrique, *Enhanced Oil Recovery - Field Planning and Development Strategies.*: Gulf Professional Publishing, 2010.
- [3] API Recommended Practice 63, "Recommended Practices for Evaluation of Polymers Used in Enhanced Oil Recovery Operations," 1990.
- [4] ASTM Standard D1681 - 05, "Standard Test Method for Synthetic Anionic Active Ingredient in Detergents by Cationic Titration Procedure," reapproved 2014.
- [5] ASTM Standard D1768 - 89, "Standard Test Method for Sodium Alkylbenzene Sulfonate in Synthetic Detergents by Ultraviolet Absorption," reapproved 2016.
- [6] ASTM Standard D3049 - 89, "Standard Test Method for Synthetic Anionic Ingredient by Cationic Titration," reapproved 2016.
- [7] ASTM Standard D4251 - 89, "Standard Test Method for Active Matter in Anionic Surfactants by Potentiometric Titration," reapproved 2016.
- [8] ASTM Standard D6173 - 97, "Standard Test Method for Determination of Various Anionic Surfactant Actives by Potentiometric Titration," reapproved 2014.
- [9] D. C. Beard and P. K. Weyl, "Influence of Texture on Porosity and Permeability of Unconsolidated Sand," *American Association of Petroleum Geologists Bulletin*, vol. 57, pp. 349-369, 1973.
- [10] A. Bera, T. Kumar, K. Ojha, and A. Mandal, "Adsorption of Surfactants on Sand Surface in Enhanced Oil Recovery: Isotherms, Kinetics and Thermodynamic Studies," *Applied Surface Science*, vol. 284, pp. 87-99, 2013.
- [11] M. Budhathoki, S. H. R. Barnee, B. J. Shiau, and J. Harwell, "Improved Oil Recovery by Reducing Surfactant Adsorption with Polyelectrolyte in High Saline Brine," *Colloids and Surfaces A: Physicochem. Eng. Aspects*, vol. 498, pp. 66-73, 2016.
- [12] P. L. Churcher, P. R. French, J. C. Shaw, and L. L. Schramm, "Rock Properties of Berea Sandstone, Baker Dolomite, and Indiana Limestone," *SPE 21044*, 1991.
- [13] F. D. S. Curbelo et al., "Adsorption of Nonionic Surfactants in Sandstones," *Colloids and Surfaces A: Physicochem. Eng. Aspects*, vol. 293, pp. 1-4, 2007.
- [14] European Standard EN 14480, "Surface Active Agents - Determination of Anionic Surface Active Agents - Potentiometric Two-Phase Titration Method," 2004.
- [15] S. Gogoi, "Adsorption-Desorption of Surfactant for Enhanced Oil Recovery," *Transport in Porous Media*, vol. 90, pp. 589-604, 2011.

- [16] M. Han, A. Fuseni, B. Zahrani, and J. Wang, "Laboratory Study on Polymers for Chemical Flooding in Carbonate Reservoirs," *SPE 169724*, 2014.
- [17] ISO Standard 2271:1989, "Surface Active Agents - Detergents - Determination of Anionic-Active Matter by Manual or Mechanical Direct Two-Phase Titration Procedure," reapproved 2016.
- [18] E. Jurado, M. Fernández-Serrano, J. Núñez-Olea, G. Luzón, and M. Lechuga, "Simplified Spectrophotometric Method Using Methylene Blue for Determining Anionic Surfactants: Applications to the Study of Primary Biodegradation in Aerobic Screening Tests," *Chemosphere*, vol. 65, pp. 278-285, 2006.
- [19] J. E. Juri, A. M. Ruiz, M. I. Hernandez, and S. Kaminszczik, "Estimation of Polymer Retention from Extended Injectivity Test," *SPE 174627*, 2015.
- [20] D. L. Kuehne and D. W. Shaw, "Manual and Automated Turbidimetric Methods for the Determination of Polyacrylamides in the Presence of Sulfonates," *SPE 11784*, 1985.
- [21] W. Kwok, H. A. Nasr-El-Din, R. E. Hayes, and D. Sethi, "Static and Dynamic Adsorption of a Non-Ionic Surfactant on Berea Sandstone," *Colloids and Surfaces A: Physicochem. Eng. Aspects*, vol. 78, pp. 193-209, 1993.
- [22] R. D. Lentz, R. E. Sojka, and J. A. Foerster, "Estimating Polyacrylamide Concentration in Irrigation Water," *J. Environ. Qual.*, vol. 25, pp. 1015-1024, 1996.
- [23] W. Lv et al., "Static and Dynamic Adsorption of Anionic and Amphoteric Surfactants with and without the Presence of Alkali," *Journal of Petroleum Science and Engineering*, vol. 77, pp. 209-218, 2011.
- [24] R. F. Mezzomo, P. Moczydlower, A. N. Sanmartin, and C. H. V. Araujo, "A New Approach to the Determination of Polymer Concentration in Reservoir Rock Adsorption Tests," *SPE 75204*, 2002.
- [25] F. Rodriguez, D. Rousseau, S. Bekri, M. Djabourov, and C. Bejarano, "Polymer Flooding for Extra-Heavy Oil: New Insights on the Key Polymer Transport Properties in Porous Media," *SPE 172850*, 2014.
- [26] J. J. Sheng, *Modern Chemical Enhanced Oil Recovery - Theory and Practice*.: Gulf Professional Publishing, 2011.
- [27] S. Solairaj, C. Britton, D. H. Kim, U. Weerasooriya, and G. Pope, "Measurement and analysis of surfactant retention," *SPE 144247*, 2012.
- [28] K. S. Sorbie, *Polymer-Improved Oil Recovery*.: CRC Press, 1991.
- [29] K. C. Taylor, "Spectrophotometric Determination of Acrylamide Polymers by Flow Injection Analysis," *SPE 21007*, 1993.
- [30] K. C. Taylor and H. A. Nasr-El-Din, "Acrylamide Copolymers: A Review of Methods for the Determination of Concentration and Degree of Hydrolysis," *Journal of Petroleum Science and Engineering*, vol. 12, pp. 9-23, 1994.
- [31] Thermo Scientific, "Acclaim Surfactant Column Product Manual," 2012.

- [32] K. Tôei, S. Motomizu, and T. Umamo, "Extractive Spectrophotometric Determination of Non-Ionic Surfactants in Water," *Talanta*, vol. 29, pp. 103-106, 1982.
- [33] K. Ueno and K. Kina, "Colloid Titration - A Rapid Method for the Determination of Charged Colloid," *J. Chemical Education*, vol. 62, pp. 627-629, 1985.
- [34] Y. E. Volokitin, I. N. Kolstov, and M. Y. Evseeva, "Experimental Studies of Surfactant Adsorption under Conditions of ASP Flooding at West Salym Field," *SPE 171223*, 2014.
- [35] W. Wang and Y. Gu, "Experimental Studies of the Detection and Reuse of Produced Chemicals in Alkaline/Surfactant/Polymer Floods," *SPE 84075*, 2005.
- [36] J. Wang, M. Han, A. Fuseni, and D. Cao, "Surfactant Adsorption in Surfactant-Polymer Flooding for Carbonate Reservoirs," *SPE 172700*, 2015.
- [37] H. Wan and R. S. Seright, "Is Polymer Retention Different under Anaerobic vs. Aerobic Conditions?," *SPE 179538*, 2016.

■